ISTANBUL TECHNICAL UNIVERSITY ★ INSTITUTE OF SCIENCE AND TECHNOLOGY

MESOPHASE PITCH DERIVED GRAPHITIC CARBON FOAM

MSc. Thesis by
Ayşenur GÜL, BSc.

Department: Advanced Technologies in Engineering

Programme: Material Science and Engineering

JANUARY 2005

İSTANBUL TECHNICAL UNIVERSITY ★ INSTITUTE OF SCIENCE AND TECHNOLOGY

MESOPHASE PITCH DERIVED GRAPHITIC CARBON FOAM

MSc. Thesis by
Ayşenur GÜL, BSc.

706021009

Date of submission: 27 December 2004

Date of defence examination: 26 January 2005

Supervisor (Chairman): Prof. Dr. M. Ferhat YARDIM

Prof. Dr. Ekrem EKİNCİ

Members of the Examining Committee Prof. Dr. Hüsnü ATAKÜL

Prof. Dr. Mustafa ÜRGEN

Prof. Dr. Sezai SARAÇ

JANUARY 2005

İSTANBUL TEKNİK ÜNİVERSİTESİ ★ FEN BİLİMLERİ ENSTİTÜSÜ

MEZOFAZ ZİFT BAZLI GRAFİTİK KARBON KÖPÜK

YÜKSEK LİSANS TEZİ
Kimya Müh. Ayşenur GÜL
706021009

Tezin Enstitüye Verildiği Tarih: 27 Aralık 2004
Tezin Savunulduğu Tarih: 26 Ocak 2005

Tez Danışmanı : **Prof. Dr. M. Ferhat YARDIM**
Prof. Dr. Ekrem EKİNCİ

Diğer Jüri Üyeleri **Prof. Dr. Hüsnü ATAKÜL**
Prof. Dr. Mustafa ÜRGEN
Prof. Dr. Sezai SARAÇ

OCAK 2005

PREFACE

During my research, I have had a great deal of help in terms of information, investigation and guidance from my dearest supervisors Prof. Dr. M. Ferhat YARDIM and Prof. Dr. Ekrem EKİNCİ. I am grateful to them for their help, supervisions, and for their patience.

I am grateful to State Planning Organization for financial support during my MSc.

I would like to express many thanks to Prof. Dr. Mustafa ÜRGEN, who is coordinator of Material Science and Engineering Program, for his advice, encouragement and support during this study.

I should thanks to technician Hüseyin SEZER for his assist during Helium pycnometry measurement and research assistant Tuncay TURUTOĞLU for his help during SEM analysis.

It is a great pleasure for me to thank Prof. Dr. Asao OYA who is the head of Department of Nano-Material Systems in Gunma University for his spiritual support, precious guidance, and generosity. He accepted me as one of members of his Carbon Group and he gave me a great courage to complete my thesis with success.

I also would like to thank Assoc. Prof. Jun-ichi OZAKI, Dr. Soshi SHIRASI, Dr. Nirav PATEL for their generosity during my research in the laboratories of Gunma University.

I also would like to special thank to my dearest brother Barbaros GÜL and other member of my family who have given me endless support all my life long.

Many thanks are also due to my dearest friends; Yasin ARSLANOĞLU, Birgül DEMİRKOL, Mehmet Özgür SEYDİBEYOĞLU, Andelip ERDOĞAN, Taner BOSTANCI, Serkan ÇAĞLI, Didem OMAY, Nagehan GENCAY, Filiz KARADAĞ, Ayhan EKŞİLİOĞLU and Melda SİPAHİ for their invaluable supports.

January 2005 Ayşenur GÜL

CONTENTS

LIST OF TABLES

LIST OF FIGURES

Page No

MESOPHASE PITCH DERİVED GRAPHITIC CARBON FOAM

SUMMARY

The recent development of new technology devices emerge the requirement of the light weight and more efficient thermal management materials. The main concept of these thermal management materials applications are high thermal conductivity, low weight, low coefficient of thermal expansion, high specific strength and low cost.

Conventional thermal management materials have centered on aluminum and copper due to its high thermal conductivity (180 W/m.K for aluminium and 400 W/m.K for copper). When the weight is taken into account, the specific thermal conductivity (thermal conductivity divided by specific gravity) is only 54 and 45 W/m.K respectively.

Carbon foam materials are used since 1960's. Existing carbon foams are used as thermal insulator or structural reinforcement until 2000. The optimization in production techniques of carbon foam resulted in high thermal conductivity low-density mesophase pitch derived graphitic foam. The pitch derived graphitic foam is used in thermal management devices such as radiator, heat exchanger.

The goal of this study is to produce graphitic carbon foam. Mesophase pitch is used for precursor. Pitch is heated above the softening point in autoclave and then pressure is applied. Green carbon foam is obtained. Then, it is stabilized and carbonized. Following these initial stages, carbon foam is graphitized up to temperature of 3000 ^{o}C. Graphitized carbon foams are characterized with the scanning electron microscopy, x-ray diffractometry, and helium pycnometry. Also thermal diffusivity of the samples are measured by laser flash apparatus.

The structures and properties of the produced graphitized carbon foams are obtained with respect to the parameters involved and further using the characterization results. The effect of foaming pressure, process temperature and polymer additives on the structure are investigated.

As a result of these experiments it is found that; the structure of the carbon foams obtained at temperatures higher than 300 ^{o}C, showed deterioration in the cell, ligaments, and junctions. Polymethyl methyacrylate (PMMA) and Polystyrene (PS) additives resulted in smoother carbon foam topography. This structural change accomplished with loss of foaming quality for the case of PS addition compared to PMMA. Higher operating pressure ended with homogeneous, interconnected, better aligned structure. Graphitized foams obtained at 68 bar have better formation in terms of interlayer spacing, stack height, crystal size and graphitization degree than other obtained foams.

MEZOFAZ ZİFT BAZLI GRAFİTİK KARBON KÖPÜK

ÖZET

Teknolojinin ilerlemesiyle ağırlığı düşük ve yüksek verimli ısıl yönetim cihazlarına duyulan ihtiyaç artmıştır. Bu ısıl yönetim uygulamalarındaki amaç yüksek ısıl iletkenliğe sahip düşük ağırlıklı, ısıl genleşme katsayısı düşük, dayanımı yüksek ve üretim maliyeti düşük tutmaktır.

Geleneksel yöntemde kullanılan ısı yönetimi yüksek iletkenliğe sahip bakır ve alüminyum üzerinde toplanmıştır (alüminyumun ısıl iletkenliği 180 W/m.K, bakırın ısıl iletkenliği 400 W/m.K). Ağırlık hesaba katıldığında spesifik ısıl iletkenliğin (ısıl iletkenlik/yoğunluk) çok düşük olduğu görülür. Alüminyumun spesifik ısıl iletkenliği 54 W/m.K iken bakır için bu değer 45 W/m.K dır.

Karbon köpüğü 1960'dan beri kullanılmaktadır. Mevcut karbon köpükleri 2000 yılına kadar ısı izolasyonunda veya yapı güçlendiricisi olarak kullanılmaktaydı. Karbon köpüğü üretim tekniklerinin daha uygun hale getirilmesiyle yüksek ısıl iletkenliğe sahip, düşük yoğunluklu mezofaz ziftbazlı grafitik köpük elde edildi. Ziftbazlı grafitik köpük radyatör, ısı değiştiricisi gibi pek çok cihazda kullanılmaktadır.

Bu çalışmanın amacı grafitik karbon köpüğü üretmektir. Mezofaz ziftin hammadde olarak kullanıldığı bu çalışmada, zift erime sıcaklığının üstünde bir sıcaklığa otoklavda ısıtılır ve yüksek basınca tabi tutulur. Elde edilen ham karbon köpüğü stabilizasyon ve karbonizasyon aşamalarından geçer. Daha sonra 3000 °C de grafitize edilir. Grafitik köpük taramalı elektron mikroskobu, x-ışını diffraktometresi ve helyum piknometresi kullanılarak karakterize edilmiştir. Ayrıca lazer flaş cihazı ile ısıl diffusivitesi ölçülmüştür.

Karakterizasyon sonuçlarına göre ise değişik proses şartlarında üretilen karbon köpüğünün yapısı belirlenmiş olur. Bu çalışmada değişik basınçlar, sıcaklıklar ve katkı maddelerinin köpük yapısına etkisi incelenmiştir.

Yapılan deney sonuçlarında, 300 °C den yüksek sıcalıklarda üretilen köpüklerinde hücre, ligament, bağlantı noktaları açısından gerileme gözlenmiştir. Polimetilmetakrilat (PMMA) ve Polistiren (PS) ilaveleriyle karbon köpüğünün yüzeyinin daha pürüzsüz olduğu gözlenmiştir. PS katkılı karbon köpüğünde (PMMA katkılı karbon köpüğüne oranla) gözenek ve hücre yapısının bozulduğu gözlenmiştir. Artan basınçla homojen, gözenekli ve düzenli bir yapıya sahip karbon köpüğü elde edilmiştir. 68 bar basınçta elde edilen karbon köpüğü, tabakalar arası mesafe, yığın yoğunluğu ve yüksekliği açısından diğer basınçlarda elde edilen köpüklere göre daha iyi sonuç vermiştir.

1. INTRODUCTION

On the fields of development of advanced materials technology has been driven by the requirement for improved more efficient and light weight thermal management materials.

Contemporary thermal management materials have centered on aluminum and copper due to their high thermal conductivity. However, in advanced device weight is significant concern. Therefore research of lighter weight thermal management materials are the interest of many researchers.

Carbon foams have been studied since 1960's [1]. Mesophase pitch-based carbon foams are proving to be popular in the field of carbon materials. Its popularity is due to producing high pore structure, high thermal conductivity and low density. Mesophase pitch derived graphitic carbon foams can be considered as an interconnected network of graphitic ligaments. Therefore graphitic carbon foams have high thermal conductivities along the ligaments of the foam. Their thermal conductivities are five times higher than copper and six times greater than aluminum.

In this study, mesophase pitch based graphitic carbon foam will be produced. The effect of different process parameters (pressure, temperature and additive) on the properties of carbon foam will be investigated by the several characterization methods.

2. GENERAL INFORMATION ABOUT CARBON AND CARBON FOAM

2.1. Carbon

Carbon is the most important element for all living organism on the Earth, because all organic compounds are composed from carbon networks. Carbon materials, which consist of mainly carbon atoms, have been used since prehistoric times in the form of charcoal. [2]

Carbon has an atomic weight of 12 and it is the sixth element in the periodic table. Three isotopes are mostly known: ^{12}C, ^{13}C, ^{14}C. Carbon-12 and carbon-13 are stable isotopes. They do not spontaneously change their structure and disintegrate. ^{12}C accounts for around 99 % of the naturally occurring carbon and is used as reference definition of atomic mass. ^{13}C is used as probe in nuclear magnetic resonance because of its magnetic moment (spin=1/2). ^{14}C is radioactive and has long half life of 5730 years and is used extensively in the dating of archaeological artifacts and as a 'label' in the study of organic reaction mechanisms. [2]

The configuration of carbon atom is shown in Figure 2.1. Carbon has four electrons in its valance shell (outer shell). Since the energy shell can hold eight electrons, each carbon atom can share electrons with up to four different atoms. It makes advantages to combine with different kind of atoms as well as it self. [3]

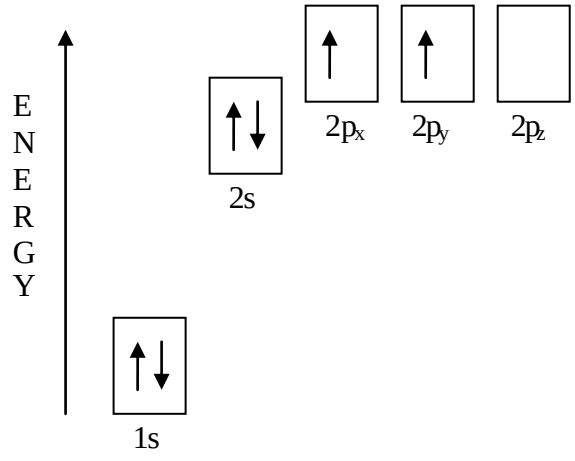

Figure 2.1 Energy levels graph of carbon atom [4]

2.2 Bonding in carbon material

Bonding in carbon compounds is explained by two principle regimes as described below:

1. σ–bonds: diamond or aliphatic type. This result in chain of carbon atoms such as polyolefine's, or three dimensional structures which are rigid and isotropic.
2. A mixture of σ and π bonds: graphite aromatic type. This results in predominantly layered structures with high degree of anisotropy.

The majority of carbonaceous materials contain examples of both bonding regimes with an immense range of complexity [3].

2.3 Crystal structures of carbon

Carbon atoms can have three different hybrid orbital, sp^3, sp^2, and sp. This variety makes carbon atomto have different forms therefore there are many kinds of carbon allotropes. Diamond, graphite and fullerene are mostly known. C-C bonds using sp^3 and sp^2 hybrid orbital was known in the construction of diamond and graphite respectively. Fullerene is constructed by combining sp and sp^2 hybrid orbital [5]

Diamond is the one of the hardest material and has no color. Its structure consists of regular three dimensional networks of sp^3 σ bonds with long range periodical repetition. Most diamond crystal belongs to cubic system. Diamond is used as an electrical insulator because of its fixed bonding electron within the diamond lattice. It is used as industrial cutting tools due to its hardness (Figure 2.2) [5, 6].

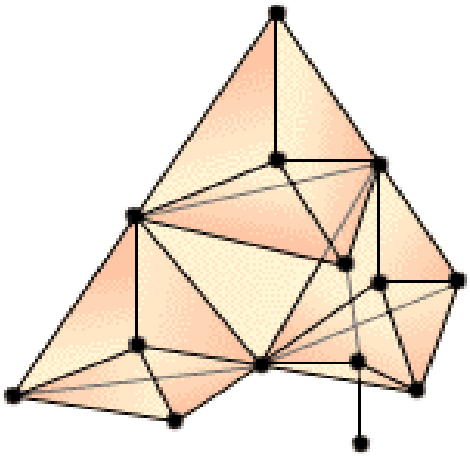

Figure 2.2 Structure of diamond [7]

Graphite structure (see Figure 2.3) has sp^2 σ and π bonds. It represents the hexagonal crystal system with the regularity of ABAB. There is a σ bond between the layers and the π bonds between the stack. The small amount of material is stacked according to the ABCABC which is known as rhombohedral form. This material accounts for less than 10% of the graphite. Graphite is a good conductor of heat and electricity. Since the energy for sliding layers over one another is low, graphite is very soft material. Thus, it used as a lubricant [3].

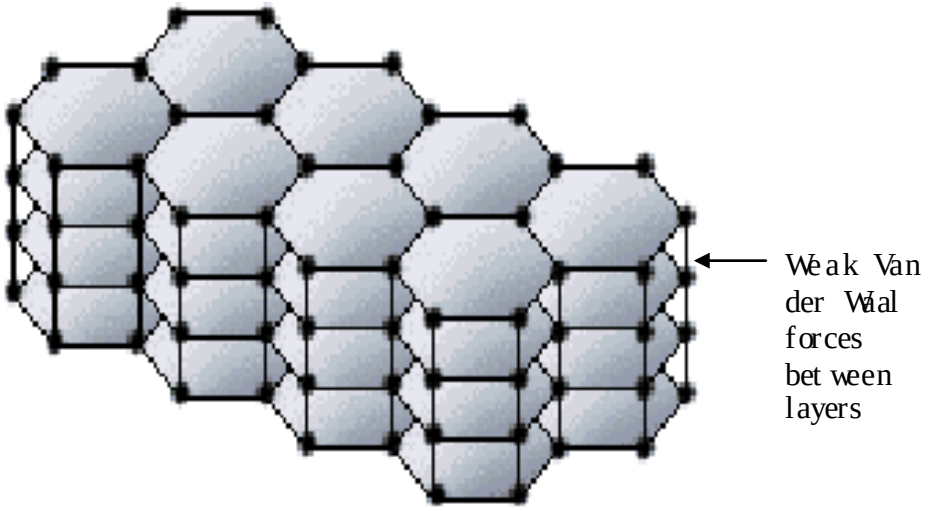

Figure 2.3 Graphite structure [7]

Fullerene (see Figure 2.4) was discovered in 1985. It is the cage molecule of carbon. The nature of bonding close to the sp^2 bond but it isn't clear. The hybridization is modification of the sp^3 hybridization and sp^2 hybridization. It means the sigma (σ) orbital don't display σ character, and the pi (π) orbital don't display π character purely. Fullerene is the one of the well known superconductive material [5].

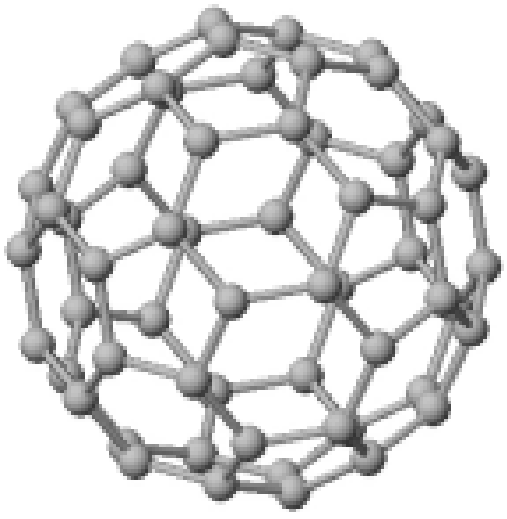

Figure 2.4 Fullerene Molecule [8]

2.4 Historical Overview of Carbon Materials

Carbon, in the form of charcoal, is an element of prehistoric discovery and was familiar to many ancient civilizations. A historical perspective of carbon and its allotropes are shown in Figure 2.5.

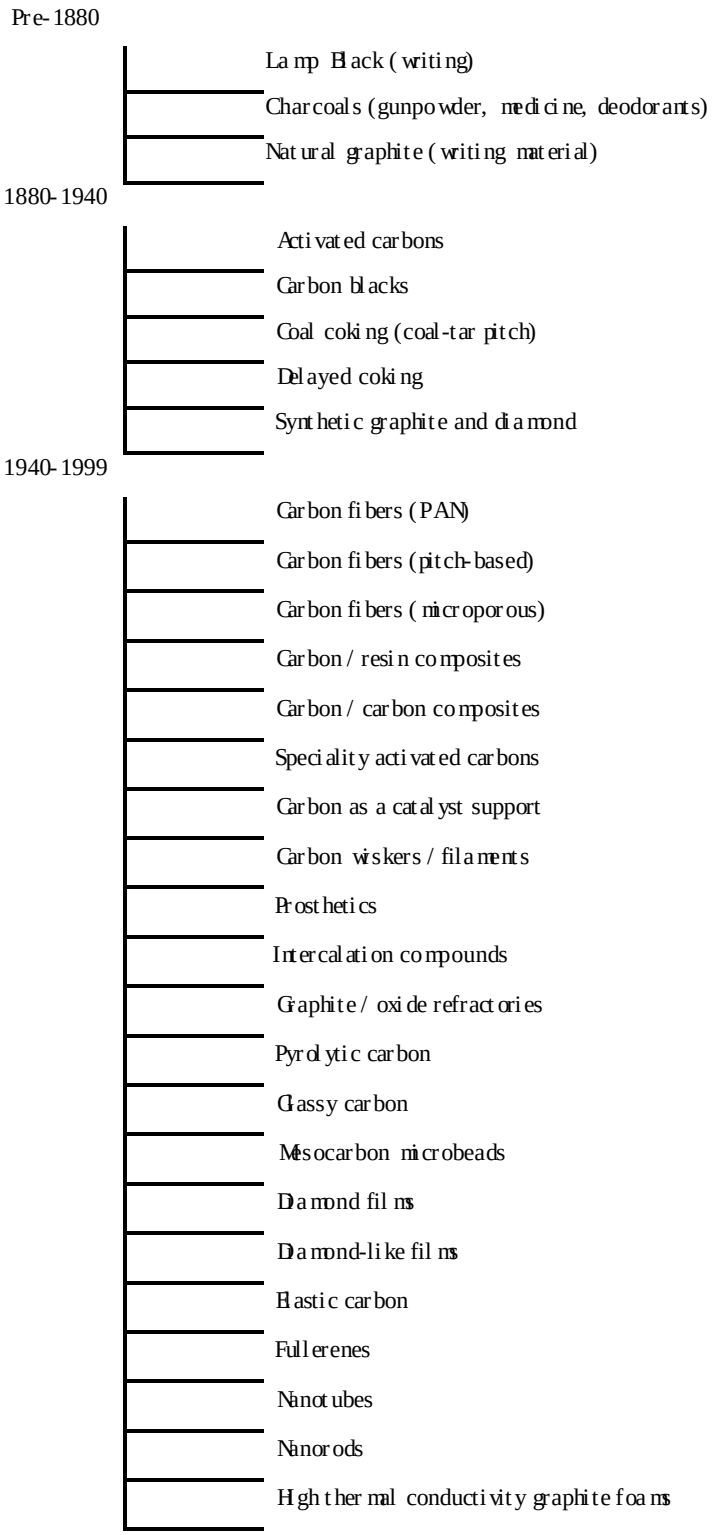

Figure 2.5 A diagram indicating the growth of carbon materials [2]

2.5 Order and Disorder in Carbon Materials

Carbon material can be classified with respect to the proportion of the ordered and disordered structure. The proportions of them are related with the properties of the material.

2.5.1 More Ordered Structures

Ordered structure can be imagining by graphite lattice. Small volumes exhibit perfect graphite crystal structure. As volume increases, the presence of defects, distortions and heteroatom destroy the regularity and produce disordered material. Layers can be slide over another layer by little amount of energy. Also twisting makes the structure parallel and equidistant layers, but with random orientation. These are called 'turbostratic' carbons. [3,9] The diamonds like parts of the most carbon materials have shorter range order than graphitic regions, although large proportions of the disordered parts are aliphatic order. Defects and irregularities can be observed in the long range orders [3].

2.5.2 Less Ordered Structures

Carbon materials can be classified by the isotropy and anisotropy. Anisotropic carbons have ordered and graphitic structure. Isotropic carbons have randomly arranged materials. The order can be increased by further heat treatment. The crystal structure changing by heat treatment is shown in Figure 2.6 [3].

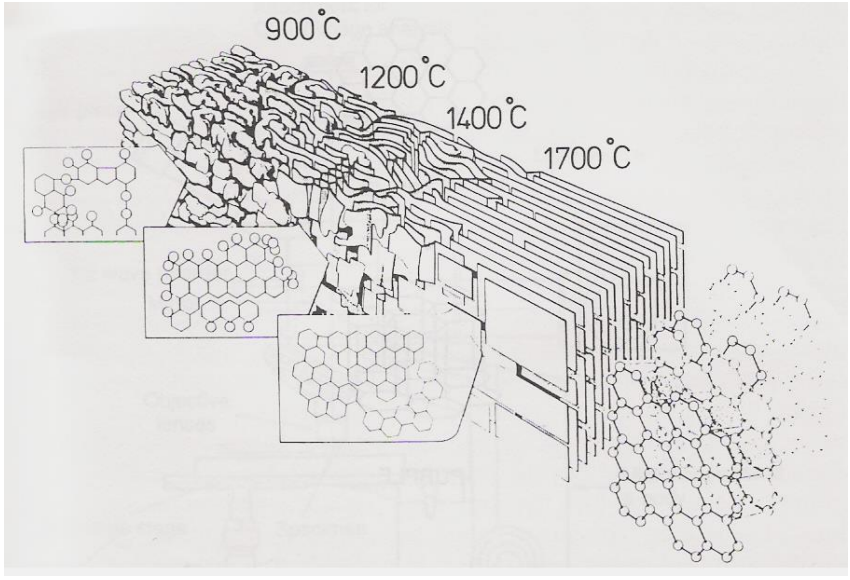

Figure 2.6 Marsh-Griffiths model of carbonization / graphitization process [3]

2.6 Carbon Forms

2.6.1 Graphitic and Non-Graphitic carbons

Graphitic carbons are all varieties of material consisting of the element carbon in the allotropic form of graphite, irrespective of the presence of structural defects. Natural graphite is a mineral consisting of carbon regardless of crystalline perfection. Some natural graphite's show a high degree of perfection but most are mined in the form of flake graphite's containing other mineral matter. Synthetic graphite is defined as a material consisting mainly of graphitic carbon, which has been obtained by means of a graphitization heat treatment of a non graphitic carbon or by chemical vapor deposition (CVD) from hydrocarbons at temperatures above 1800° C [10].

Non-graphitic carbons are all varieties of substances consisting mainly of the element carbon with two-dimensional long range order of the carbon atoms in planar hexagonal networks, but without any measurable crystallographic order in the c-direction. Many non-graphitic carbons can be converted to graphite by graphitization heat treatment to above 2200 ° C

2.6.2 Graphitizable and non Graphitizable Carbons

Non-graphitizable carbons (see Figure 2.7) can not be transformed into graphitic carbon solely by heat treatment at temperatures of 3000° C or above under atmospheric or lower pressures. Non Graphitizable carbons are produced from wood, nutshells and non fusing coals. During heat treatment, their macromolecular structure does not change. Fusion can not take place only small molecules leave from the structures, and at the same time more cross linking structure occurs [10].

Graphitizable carbons can pass fluid stage during the heat treatment. Molecules can grow and large aromatic molecules can be formed. Thus they align with each other so graphitic structure can be developed [10].

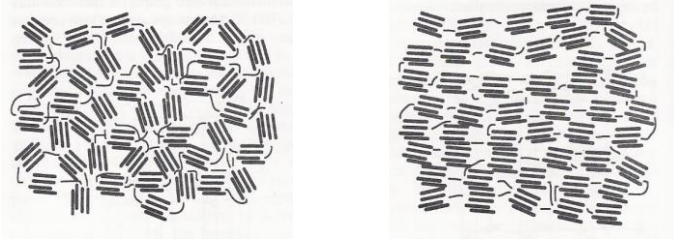

Figure 2.7 Schematic representation of nongraphitizable (left) and graphitizable carbon (right)

2.7 Carbon Foam

Carbon foam has been produced from different kind of precursors since 1960's such as synthetic mesophase pitches [11,12], coal tar and petroleum pitch [13], coal [14], polyacrylonitrile (PAN) [15], polyurethane [16], vinylidine chloride polymer [17], phenolic polymer [18] and pyrolizable organic compound such as sugar or cellulose [19].

The carbon foam is an alternative material to traditional material in many applications due to its unique properties. For example, carbon foam is used as insulator and conductor material according to the operating temperature. Carbon foam has low thermal conductivity when it is produced below the temperature of 1000 °C. In contrast, carbon foam high thermal conductivity when it is produced above the temperature of 2500 °C. Carbon foam conducts heat six times faster than copper and four times faster than aluminum [20]. The thermal properties of the carbon foam compared to other thermal management material are illustrated in Table2.1.

Table 2.1 Thermal properties of pitch derived carbon foams compared to other thermal management materials [21]

Material	Specific gravity	Thermal Conductivity		Specific thermal conductivity*	
		In-plane (W/m.K)	Out-of-plane (W/m.K)	In-plane (W/m.K)	Out-of-plane (W/m.K)
ARA24 derived foam-D	0.57	149	149	261	261
Conoco-derived foam-D	0.59	134	134	227	227
Typical 2-D carbon carbon	1.88	250	20	132	10.6
EWC-300/Cyanate Ester	1.72	109	1	63	0.6
Copper	8.9	400	400	45	45
Aluminum	2.77	150	150	54	54
Aluminum honeycomb	0.19	-	~10	-	52
Aluminum foam	0.5	12	12	24	24

*defined as thermal conductivity divided by specific gravity

Carbon foam has nearly 90 % open pore structure. The density of carbon foam is ranging from 0.20 g/cm^3 to 0.6 g/cm^3. Carbon foam has high porous structure and uniform pore size distribution (average between 10 and 500 microns) [13].

Carbon foam shows highly ordered graphite properties when it is graphitized. It exhibits average interlayer spacing as low as that of perfect graphite [21]. For instance, carbon foams produced by Klett et al.[22] has a 0.336 nm inter layer spacing and 203.3 nm coherent length (La) and 442 nm stacking height (Lc).

2.7.1 History of Carbon Foam

Walter Ford [1] first developed carbon foam in the late 1960's. This initial carbon foam was produced by carbonizing thermosetting polymer foams to obtain reticulated vitreous (glassy) carbon foam which is shown Figure 2.8.

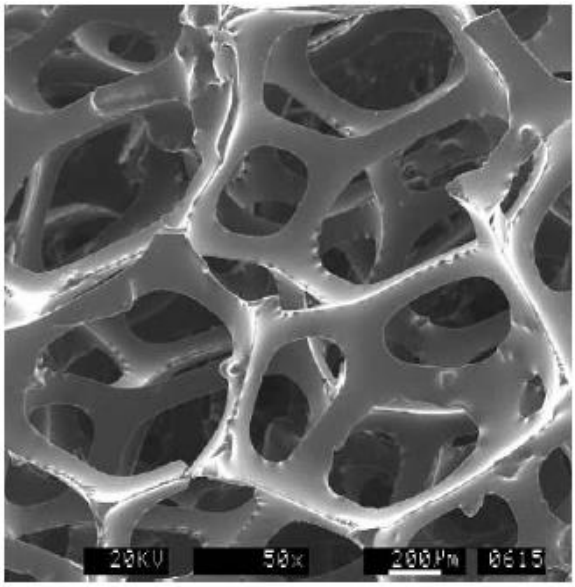

Figure 2.8 A Typical RVC foam[21]

Googin et al. [26] produced carbon foam by polymerization of furfuryl alcohol and urethane to get partially cured urethane foam in 1967. It was the first process to controlling the structure and material properties of carbon foam.

Researches focused on variety of applications of carbon foam. Carbon foam was used as electrode, insulator, filter, catalyst bed and catalyst support. In addition, carbon foam was used as the template for many of the metal. In 1970's and 1980's, alternative precursors and processing conditions were explored for producing carbon foam and modifying its properties [16, 17, 23, 24].

In 1976, Raley et. al. [17] used vinylidine chloride polymers with ammonia to derive carbon foam. This carbon foam had been used as a catalyst support and filter material for gases, such as cigarette smoke and liquids.

In 1981, Bonzom et. al. [13] developed carbon foam from petroleum and coal tar pitch. The carbon foam was used for thermal and sound insulating.

In 1988, Hopper [18] dissolved pulverized sodium chloride particles and phenolic polymeric resin into tetrahydrofuran (THF) as a precursor of carbon foam.

In the early 1990's mesophase pitch derived carbon foam was discovered [25]. This work was focused on the developing a highly structural light weight material which exhibits very high specific thermal conductivity.

In 1997, Klett, J. [22, 27-29] at the Oak Ridge National Laboratory (ORNL) reported the first graphitic foams with bulk thermal conductivities up to 180 W/m.K. They used naphthalene derived mesophase pitch as a precursor. Due to high bulk thermal conductivity, the graphitic carbon foam is a potential material as thermal management materials.

2.7.2 Preparation and Characteristic of Mesophase Pitch Derived Graphitized Carbon Foam

2.7.2.1 Mesophase Pitch

The mesophase phenomenon is discovered in 1965 by Brooks and Taylor [30]. Mesophase means sphere and mosaic substances that form before the solidification. When hydrocarbon is heated under inert atmosphere, it condenses to large planar molecules. As the molecules grow, they nucleate and grow a liquid crystal phase, called the mesophase. The liquid crystal phase consists of stacking planar molecules that are footprint of the graphitic pellets [30].

The mesophase pitch based carbon foam was produced at the Wright Patterson Air Force Base Materials Lab in 1990's [31]. It is a synthetic naphthalene derived pitch, which is 100% anisotropic mesophase.

Mesophase pitch is derived from various precursors such as petroleum and coal tar and other synthetic precursors. Mesophase pitches derived from synthetic precursors, such as Mitsubishi AR pitch which is prepared by the catalytic polymerization of

naphthalene using HF-BF_3 catalyst [32, 33], have more homogeneous compositions compared to mesophase pitch derived from petroleum and coal tar pitch [34]. Figure 2.9 schematically shows the presentation of the structures of Mitsubishi AR and typical petroleum mesophase pitches [21].

Synthetic Mesophase pitch is preferable precursor for high thermal conductivity carbon foam materials. When a synthetic mesophase pitch is used, the domains are stretched along the cell walls of the foam structure and thereby produce a highly aligned graphitic structure parallel to the cell walls [11]

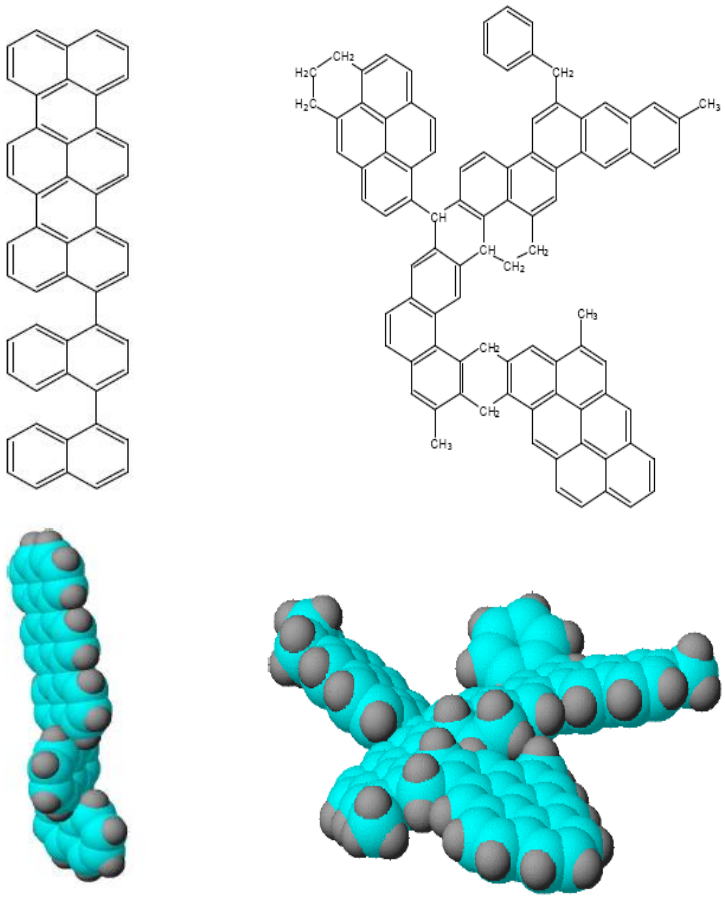

(a) (b)

Figure 2.9 Structure of mesophase pitch (a) AR mesophase pitch (b) Atypical petroleum mesophase [21]

2.7.2.2 Foaming Mechanism

While mesophase pitch is heated, mesophase molecules begin to enlarge and weaker hydrogen bonds decompose. Volatiles coalesce into larger bubbles while the preferred orientation occurs in the pitch. Mesophase molecules begin to align on the surrounding of the bubbles. High molecule weight compounds impede

the flow of bubbles to the surface. At the same time, there is additional stress on the pitch due to the applying pressure. Bubbles enlarge in the depressurization step (see Figure 2.10). After the pressure release, they rapture (like boiling water) and interconnected pores occur

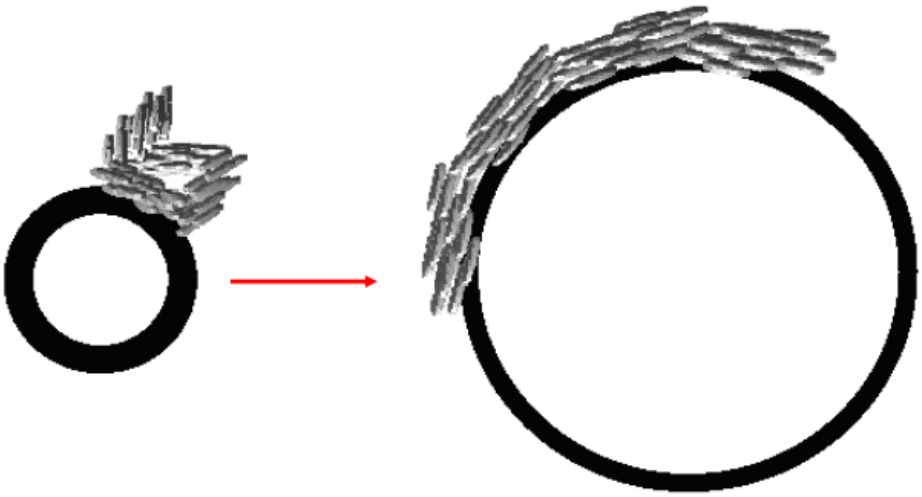

Figure 2.10 Bubbles growth under applied pressure [35]

The related terminology is indicated in the Figure 2.11 for a better understanding of the evaluation of foam. As it can be seen from the figure, cell has a spherical geometry with open pores. The number of the pores generally varies between one and four. These pores are interconnected to other cells. Interlayer between the cells is defined as ligaments. This is the part where rod-like mesophase molecules aligned and layered which causes graphitic structure at the further step of heat treatment. Junctions are located between three or more cells. Non uniform elongated region inside the cell are defined as cracks. The cracks affect the strength of the material.

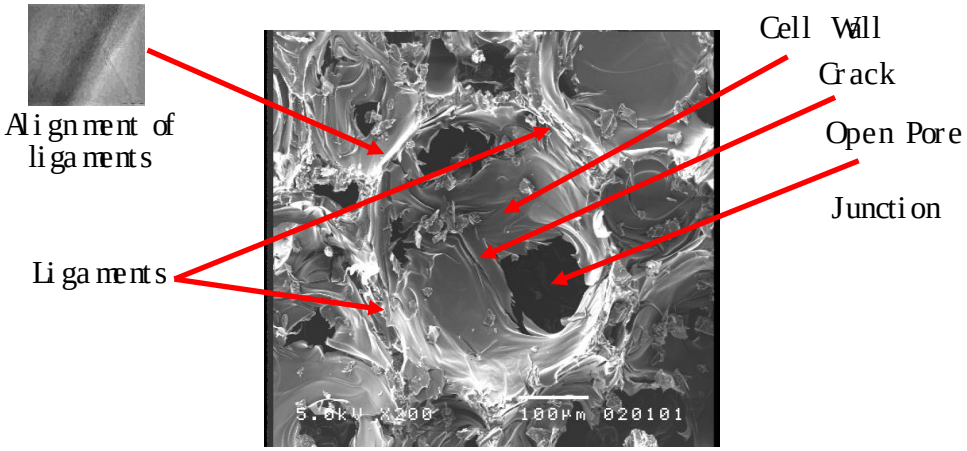

Figure 2.11 The terminology used for SEM photographs of carbon foam

2.7.2.3 Stabilization of Carbon Foam

Stabilization is described as promotion of cross linking between molecules and the removal of smaller molecules by decomposition. Stabilization includes both oxygen diffusion and oxidative reactions. Oxygen diffuses to reaction sites and product gases must diffuse out [36, 37].

Thermo gravimetric analyses of the stabilization process indicate that competing chemical processes involve both weight gain and weight loss. Weight gain predominates at lower oxidation temperatures and shorter periods of time. However, weight loss predominates at higher oxidation temperatures and longer periods of time. The weight gain period is accompanied by the production of H_2, H_2O, whereas the weight loss period is accompanied by the production of CH_4, CO and CO_2 [38, 39].

Relative rates of oxygen diffusion and oxidation reactions depend on reactivity of precursor, temperature, sample thickness and reactivity of oxidants. Stabilization reactions begin with the aliphatic side chains. Then, aromatization and cross linking are followed. Stabilization influences the performance of resulting product. Insufficient stabilization allows deformation after carbonization. Excessive stabilization causes decomposition of introduced oxygen group and more defects [40-42].

2.7.2.4 Carbonization of Carbon Foam

Carbonization is a pyrolysis process to increase content of the element carbon at inert atmosphere. The precursor is heated slowly in an inert environment. The organic material is decomposed into a carbon residue. Volatile compounds diffuse out structure. Weight loss occurs during the carbonization stage [43, 44]. Several reactions such as dehydrogenation, condensation and isomerization take place at the same time in the carbonization process. Lower heating rates and longer soaking times reduce carbonization yield during carbonization [43-45].

2.7.2.5 Graphitization of Carbon Foam

Graphitization is the transformation of non graphitic carbon into graphitic carbon by means of heat treatment at temperatures between 1700 ^{o}C and 3000 ^{o}C [46]. During graphitization, crystal size increases from 50 A^{o} to 1000 A^{o} and interlayer

spacing decreases from 3.44 A^o (amorphous carbon interlayer spacing) to the 3.35 A^o (graphitic carbon interlayer spacing). Graphitization involves displacement and rearrangement of planes and small groups of planes to achieve three dimensional ordering [47].

The mechanism is schematically explained in Figure 2.12. Basic structural unit (BSU), is a parallel stack of two or four layer planes each containing less than 10-20 aromatic rings. At stage 1, up to 1000 ^oC heat treatment temperature (HTT), the carbon contains flat BSU with a high degree of disorientation. Between 1000 and 1500 ^oC (stage 2), the BSU grow thicker and columnar arrays look like stuck of coins. In stage 3, around HTT= 1500-2000 ^oC, the disorientation between the columns of BSU decreases, carbon layers planes can form by coalescence of adjacent BSU. At the final stage, above 2000 ^oC, perfect carbon layer planes are produced. Formation and growth of graphite crystallites occur [5].

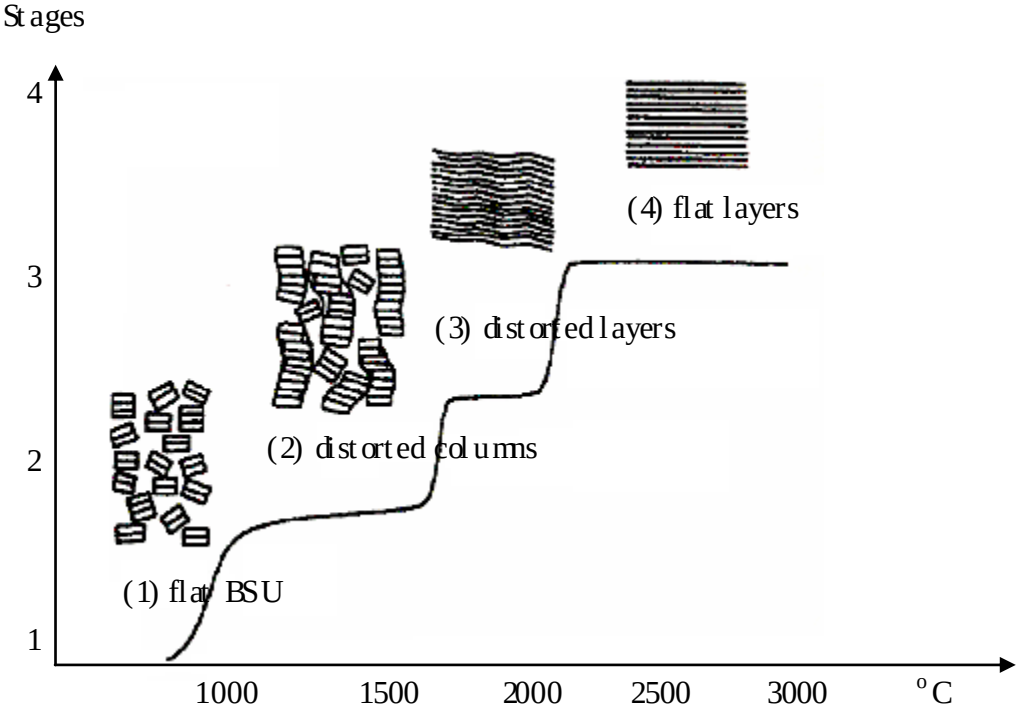

Figure 2.12 The mechanism of graphitization [5]

2.7.2.6 The Role of Structure on the Thermal Conductivity of Graphite Foam

Heat is transferred in the solid by two mechanisms. These are electrons and phonons. The method for assessing the mechanism of thermal conductivity depends on calculation of the Wiedmann-Franz ratio as function of temperature:

$$\text{Wiedman - Franz Ratio} = \frac{\text{Thermal Conductivity} \times \text{Elecrical Resistivity}}{\text{Temperature}} \qquad (2.1)$$

Thermal conductivity is controlled by the electrons near the Wiedmann-Franz ratio. Carbon based materials have very distinctive ratios from Wiedmann-Franz ratios; therefore lattice vibrations (phonons) dominate thermal conductivity [48, 49]. Phonons are the thermal waves that transfer heat energy format the one end of the lattice to other end like Mexican wave [50].

Heat transfer is fast through the graphite lattice due to very stiff nature of covalent bonds. When phonons reach defects and curvatures in the structure, the vibration of atoms is interrupted and the phonon is scattered. Also heat transfer is affected by the phonon-phonon interactions and impurities [51]

At low temperatures, there are few phonons so that phonon interacting is low. The energy of phonon is small and therefore the wavelength is large. As a consequence, the phonons are not easily scattered by impurities and imperfections (see Figure 2.13). In contrast, the probability of the interaction between phonons increases at high temperatures. Also wavelength is short which means that the phonons interact strongly with impurities (see Figure 2.12). Mean free path of the phonons increases as the temperature decreases. Consequently, thermal conductivity reduced to zero as the temperature increases. [50]

(a) (b)

Figure 2.13 Schematic diagrams showing the interaction of phonon with an impurity (a) Low Temperature, (b) High temperature [50]

2.8 Application Areas of Carbon Foam

Heat exchangers and heat sinks are used for thermal management. Heat exchangers transfer heat energy from one area to another, and heat sinks dissipate heat into the air. Conventionally, aluminum and copper heat exchangers and heat sinks are

superior for most of the areas. Carbon foam are the alternative of them by the having light weight and high thermal conductivity [52, 53, 54].

2.8.1 Radiators

Carbon foam core radiator removes more heat aluminum core radiator at the same size (see Figure 2.14). Carbon foam can be used for taking away heat from the fuel cell. Therefore, car has light weight and small size. If the size of the car is reduced, the car will not have to push as much air in front of the motion. It helps more efficient fuel usage and makes car lighter. Car will go faster and pollute atmosphere less due to aerodynamic design. For example, a radiator (see Figure 2.15) was designed for a racing car that can dissipate up to 33 kW in a volume 30 % less than a typical radiator. This reduced size will allow for better aerodynamics, resulting in more than a 4 mph gain on the super speedways. In heavy vehicles, the effect of the radiator in the front creates significant drag, accounting for up to 12 % of the fuel use at highway speeds. Clearly, a smaller radiator will allow the redesign of the front cab and dramatically improve efficiency [52].

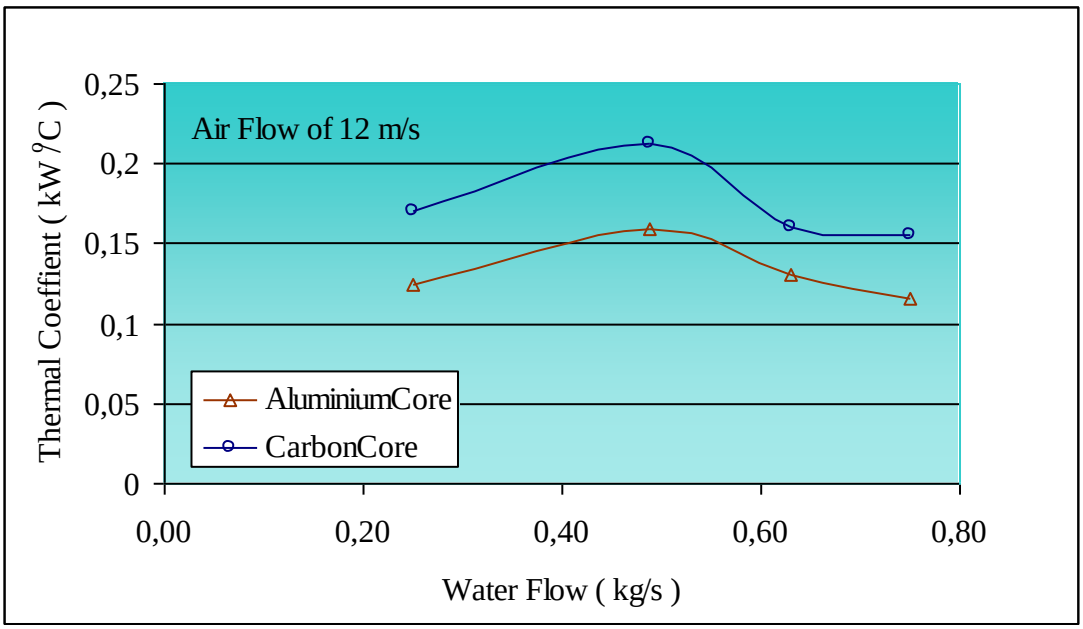

Figure 2.14 Efficiency of radiators [52]

Figure 2.15 Picture of modular radiator with heat dissipation capacity of 33 kW[52]

2.8.2 Personal Cooling Devices

A personal cooling system being developed by researchers at the Department of Energy's Oak Ridge National Laboratory (ORNL) The system is developed for fighter pilots, racing car drivers and fire fighters. These devices remove heat formthe body and help to take cooled air to breathe [53].

Figure 2.16 Graphite foam cooler [52]

2.8.3 Computer Chip Cooling

Current computer chips are placed printed side up in a ceramic package with "over-the-top" wire bonds. Unfortunately, this design is not suited for significant heat dissipation through the top of the package to a standard heat sink as there is an insulating air gap between the silicon chip and the ceramic package [54]

In cooperation with the National Security Agency (NSA) researchers at ORNL have studied on new design for cooling electronic computer chips which is called "flip-chip". In this design, the silicon chip is inverted with the smooth

back of the printed chip oriented towards the top of the package. A heat spreader is attached directly to the silicon chip and immersed in an evaporative cooling fluid (see Figure 2.16). The limitations of this design are the surface area and thermal conductivity of the spreader mounted to the back of the chip. [54]

The spreaders utilized by the NSA are polycrystalline diamond wafers with thermal conductivities up to 1600 W/m.K (more than 4 times that of copper). However, as a result of the limited surface area of the diamond spreader, the maximum power density achieved without overheating the system was 28 W/cm^2 [54].

When the diamond spreader was replaced with ORNL's graphite foam, a power density of 100 W/cm^2 was attained without overheating the system. ORNL's foam has higher power density more than %350 of the current design. [54]

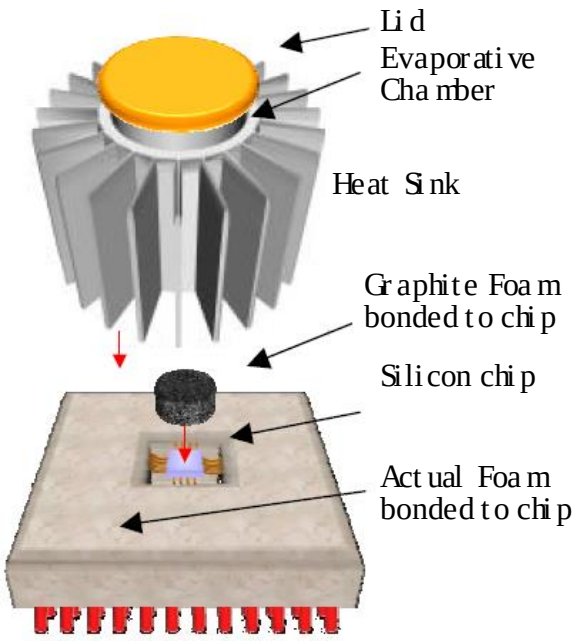

Figure 2.17 Evaporative cooling system mounted on chip package [52]

3. EXPERIMENTAL

In this research, 100% Mitsubishi AR naphthalene based synthetic mesophase pitch was used to produce graphitic foam. All foam samples were stabilized at 310 °C, and carbonized at 1050 °C and then graphitized at 3000 °C. In order to understand the fundamental characteristic of the foam structure and graphitic morphology, samples were examined by using a scanning electron microscopy (SEM), x-ray diffractometry, and helium pycnometry. In addition, thermal diffusivity is measured by laser flash diffusimetry.

3.1 Precursor for Carbon Foam Production

Mesophase pitch (Figure 3.1) was provided by Mitsubishi Gas Chemical Corp., Tokyo, Japan. The pitch; namely Mitsubishi AR mesophase pitch was produced by catalytic polymerization of naphthalene with the aid of HF-BF_3 catalyst. Naphthalene is aromatic hydrocarbon, so it is called as a synthetic mesophase pitch. Properties of AR mesophase pitch are given in Table 3.1

Figure 3.1 Mesophase Pitch

Table 3.1 Typical properties of AR pitch [39]

Physical Properties	
Appearance	Black pellets (25°C)
Bulk Density (g/cm³)	0.70 ± 0.3 ; pass: 0.69
Specific Gravity (25°C)	1.23
Specific Heat (cal/g·°C)	0.65
Softening Point (°C)	285 ± 5 ; pass: 282.9
Mesophase Content (%)	100
Hydrogen/Carbon (atom/atom)	0.58-0.64
Flash Point (°C)	> 300
Ash (ppm)	< 20
Solubility (%)	
Water Soluble	0
Benzene Soluble	35-44
Pyridine Insoluble	40-50
Coking Value (%) at 1 hr, 600°C	
1 atm	80-85
30 atm	90-95
Toxicological Information	
Acute Oral LD50 (rat)	> 5000 mg/kg
Skin Irritation	slightly irritating
Mutagenicity (Salmonella)	negative
Mutagenicity (E.coli)	negative

When using mesophase pitch as a precursor for making advanced carbon materials and carbon/carbon composites, the viscosity of the mesophase is a very important factor. If the viscosity is too high, the mesophase pitch does not impregnate well into carbon preform. The mesophase pitch flows in a liquid state above its softening point, maintaining the molecular ordering in a certain temperature range. Viscosity of the mesophase pitch is dependent on temperature and shear [32]. The viscosity curve of AR pitch is shown in Figure 3.2 and the processing window is presented in Figure 3.3

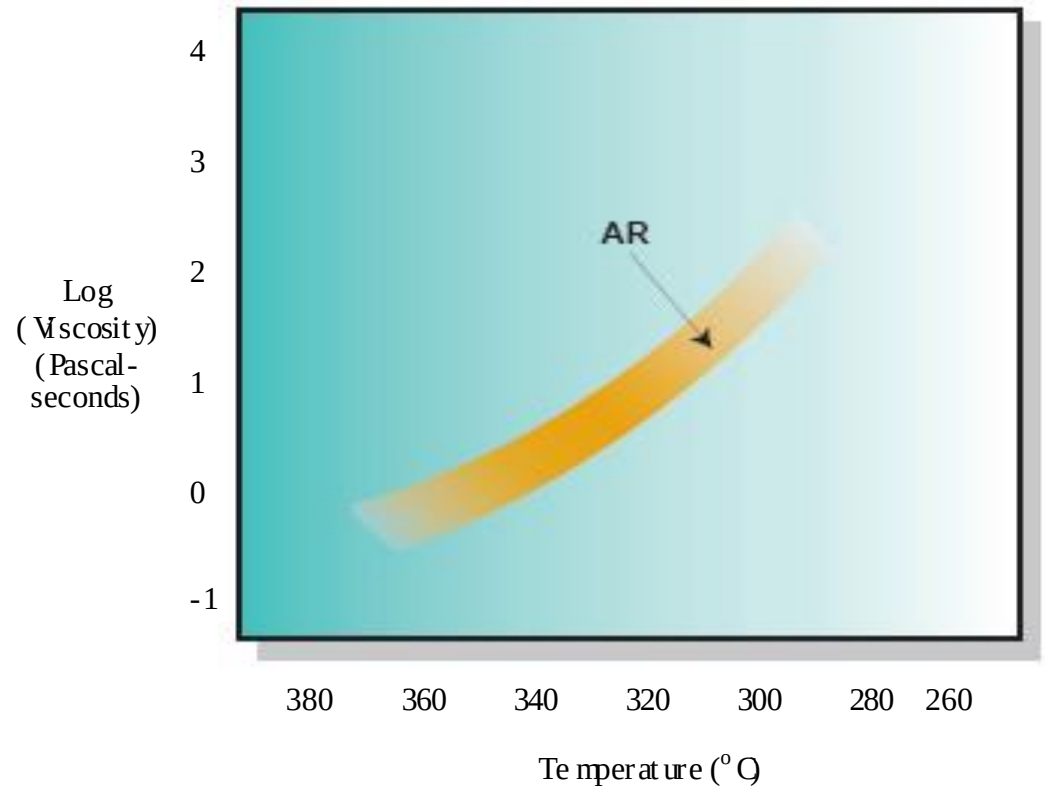

Figure 3.2 Variation of viscosity of AR pitch as a function of temperature [32]

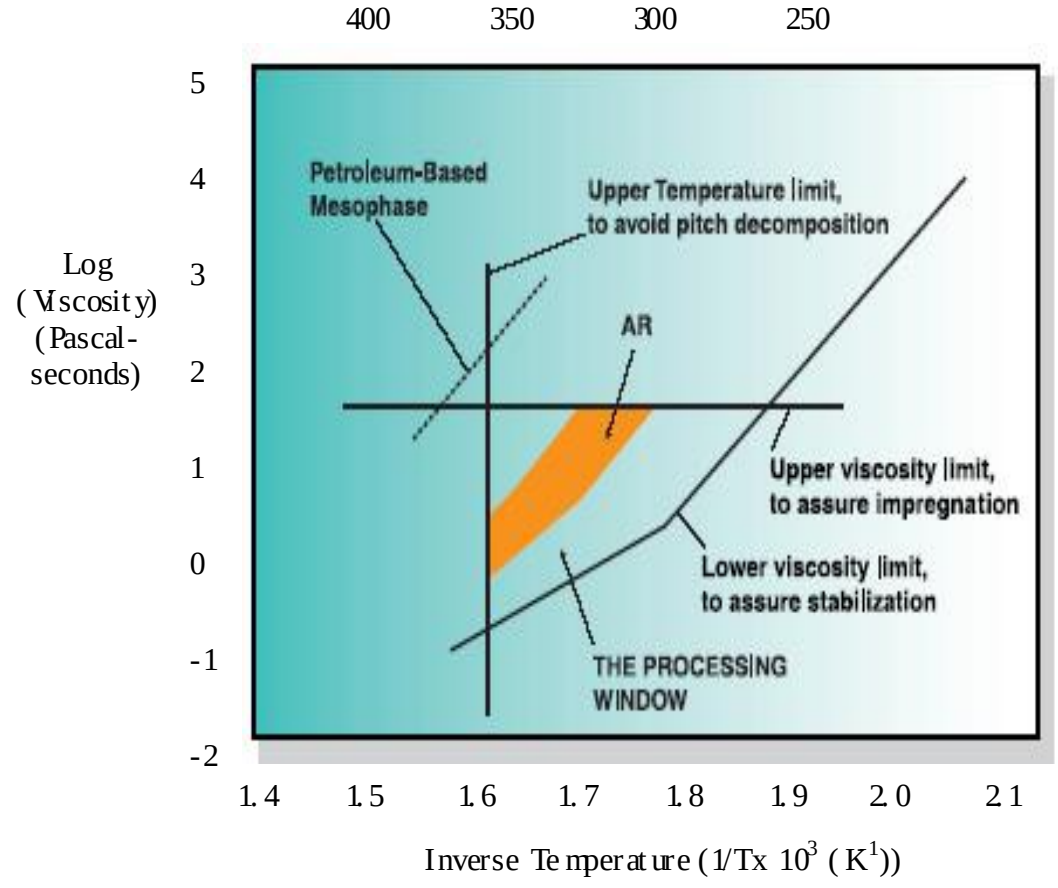

Figure 3.3 Evaluation of AR pitches by the processing window [32]

3.2 Experimental Procedure

Pitch pellets are placed in aluminum mold. The mold is introduced in an autoclave. Autoclave is stainless steel high temperature-high pressure vertical vessel in form of cylinder. Maximum allowable working temperature and pressure are 300° C and 200 bars, respectively.

Before experiment started, air in the system was purged out with nitrogen at the pressure of 5-10 bars. This sweeping process was repeated at least three times to ensure the removal of air from the autoclave. After sweeping was completed, Nitrogen was vacuumed from the system. Then, autoclave was heated above the softening point of the mesophase pitch. After achieving requested temperature, 15 minutes of soak time was applied for homogeneous thermal stability. Later nitrogen was applied to gradually build up to pressure to the desired level in a 20 minutes period and then the pressure was released to the atmospheric pressure rapidly, thereby providing means for volatiles removal which makes the porous foam. Furthermore, the autoclave was cooled to ambient temperature where the foam sample is removed.

The subsequent step was stabilization of porous foam. The stabilization step was realized in a horizontal tube furnace. The porous foams were installed at the center of the furnace and stabilized in the dry air atmosphere with a flow rate 0.5 L/min. For stabilization the samples were heated to 185° C from ambient temperature with a heating rate of 1° C/min. After a soak time of 5 hours at 185° C, the samples were heated to 275° C with a heating rate of 0.5° C/min and 5 hour soak time was applied at this temperature. Finally, the samples were heated up to 310° C with a heating rate of 0.12° C/min to terminate the heating regime and 2.5 hour of soak time was applied at this temperature. The system was cooled to room temperature with a cooling rate of 0.8° C/min. The heating regime of the stabilization process is given in Table 3.2.

Table 3.2 Heating regime of stabilization process

Temperature (°C)	Heating or cooling rate (°C/minutes)	Holding Time (Hour)
25	-	-
185	1	-
185	-	5
275	0.5	-
275	-	5
310	0.12	-
310	-	2.5
25	0.8	-

The stabilized foams were carbonized under nitrogen atmosphere. During carbonization in the first step the stabilized foams were heated to 310°C from room temperature with a heating rate of 1°C/minute. A soak time of one hour applied at this temperature. At the second step heating the samples were heated up to 750°C with a heating rate of 0.5°C/minutes and one hour soak time was is applied at this temperature. Finally the samples were heated to 1050°C with a heating rate of 0.5°C/ minutes and 2.5 hour soak time was applied at the final temperature. The carbonized foam samples were cooled to room temperature with a cooling rate of 0.8°C/ minutes. The carbonization procedure are shown in Table 3.3

Table 3.3 Heating regime of carbonization process

Temperature (°C)	Heating or cooling rate (°C/minutes)	Holding Time (Hour)
25	-	-
310	1	-
310	-	1
750	0,5	-
750	-	1
1050	0,5	-
1050	-	2.5
25	0,8	-

The carbonized foams samples were graphitized under inert atmosphere. Carbonized foams were heated immediately to 1300 °C. Heating rate of 0.3 °C/min was applied between 1300 °C and 1310 °C. A soak time of 39 minutes was applied at this temperature. Next, the samples were heated to 2000 °C with heating rate of 11.5 °C/min. Following this step, the samples were heated to 2800 °C with the heating rate of 13.3 °C/min. At the last step the sample are heated to 3000 °C with the heating rate of 3.3 °C/min and one hour soak time is applied at this temperature. The samples were cooled to 1300 °C with a cooling rate of 15 °C/min. Later, samples were cooled down to room temperature with cooling rate of 5.3 °C/min. Graphitic carbon foams obtained were characterized by several methods. Table 3.4 shows graphitization of the procedure used in this study.

Table 3.4 Heating regime of graphitization process

Temperature (°C)	Heating or cooling rate (°C/minutes)	Holding Time (min)
1300	-	-
1310	0.33	-
1310	-	39
2000	11.50	-
2800	13.33	-
3000	3.33	-
3000	-	60
1300	15.04	-
25	5.31	-

3.3 Blending Polymer

Polymer blend technique has been widely used in literature for improving some properties of carbon fiber materials [55, 56]. In order to investigate the effect of Polymethyl methacrylate (PMMA) and Polystyrene (PS) addition on the interconnected pore structure and cell formation of carbon foams, these additives are blended with various proportions to mesophase pitch.

PS and PMMA were purchased from Wako Pure Chemicals Co. Mesophase pitch and polymer were blended in the several weight ratios and dissolved in the tetrahydrofuran (THF). Excess THF was removed from the mixture by rotary evaporator.

After removal of the solvent from the mixture; sample was dried in vacuum oven for a night. As a result pitch-polymer blend is obtained. The blend is installed in a mold and same procedure (which is explained in section 3.2) was followed for the production of carbon foam is followed as explain in the section of 3.2.

PS was blended with pitch at the mixing ratio of 10%, 20%, 30% and PMMA was blended with pitch at the mixing ratio of 10%, 20%, 30%. Carbon foam obtained from 10% PS ratios and 20% PMMA ratios had large holes and irregular structure. Therefore these samples were not evaluated. Discussions and presentations in this section are therefore on the foams blended with 30%, 20% PMMA and 10%, 30% PS. The structure of THF, PS and PMMA molecules are shown in Table 3.4.

Table 3.5 Structure of THF, PMMA and PS

Molecule		
THF (Tetra hydro Furan)	C_4H_8O	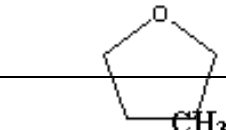
PMMA (Polymethyl methacrylate)	$C_5H_8O_2$	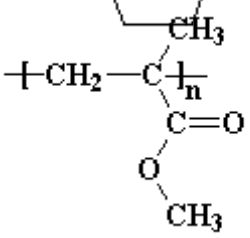
PS (Polystyrene)	C_8H_8	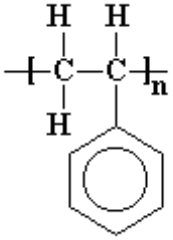

3.4 Characterization Techniques for Carbon Materials

Characterization of the structure and texture of carbon materials are essential and important for assigning proper utilization and understanding their structures. Before discussing the graphitic foam material, fundamental techniques for the characterization of the structure and texture of carbon foam are explained below

3.4.1 Thermal Diffusivity Measurement

The thermal diffusivity values can be converted to thermal conductivity using the specific heat (C_p) and density (ρ). The calculation of the thermal conductivity is realized by using the following equation:

$$\lambda(T) = \alpha . \rho . C_p \qquad (3.1)$$

The specific heat, Cp, is calculated from the following equation taken from ASTM C781 [57] which is valid from 300 to 3000 K.

$$C_p = 8.426x10^{-18}T^6 - 4.300x10^{-14}T^5 - 1.42510^{-10}T^4 + 1.35310^{-06}T^3 - 3.76510^{-03}T^2 + 4.796T - 428.1 \qquad (3.2)$$

In this method, a short pulse (less than 1 millisecond) of heat is applied to the front face of a specimen using a laser flash, and the temperature change of the rear face is measured with an infrared (IR) detector [58]. The thermal conductivities of the carbon foam samples were measured by The LFA 427 apparatus.

3.4.2 X-Ray Diffractometry

X-ray diffraction is one of the fundamental techniques to characterize crystal structure. The technique provides a measure of the amount of ordered materials and give an indication of the size of crystallites which make up the ordered structure.

When a beam of chromatic x-radiation is directed at a crystalline material, diffraction of the x-rays is observed at various angles with respect to primary beam. The relationship between the wave length of the X-ray beam (λ), the angle of diffraction (2θ), and the distance between each set of atomic planes of the crystal lattice (d), is given by the Bragg equation [59, 60]

$$n.\lambda = 2.d.\sin\theta \qquad (3.3)$$

In equation 3.3, n denotes the order of diffraction. Using this equation, the interplanar distances of crystalline material under study can be calculated. The interplanar spacing depends on the arrangement of atoms in the crystal unit cell. The intensities of the diffracted rays are function of both the diffraction power and the placement of the atoms within the unit cell [59, 60].

The broadening of the diffraction peaks allows an estimation of the mean particle size. The approximate crystallite size (t) can be calculated from the amount of broadening (β), using Scherrer equation:

$$t = c.\lambda / \beta.\cos\theta \qquad (3.4)$$

Where c is the cell dimension, λ is the X-ray wavelength and 2θ the scattering angle and β is the amount of broadening due to sample [60, 61]. The carbon foam samples were characterized with Rigaku Multiflex X-ray Diffractometer.

3.4.3 Scanning Electron Microscopy

Scanning electron microscope (SEM) has been commonly used to observe the morphology and surface of the materials. SEM operates by focusing an electron beam passing through an evacuated column on the specimen surface using electromagnetic lenses. The beam is raster scanned over the surface of the specimen in synchronism with the beam of a cathode ray tube (CRT) display screen. Inelastically scattered secondary electrons emitted from the sample surface are collected by scintillator-counter and the signal formt his used to modulate the brightness of the image on the CRT. Differences in secondary emission result from changes in surface topography. If the elastically (backscattered) electrons are collected, an image can be formed from the contrast resulting from compositional differences across the surface of the specimen [61]. In this study, Scanning Electron Microscope studies are carried out on JEOL JSM-5100

3.3.4 Helium Pycnometry

The skeleton density, which is defined as the structural or solid density, is determined with helium pycnometry. In this method, it is assumed that helium enters the smallest pores present, without being adsorbed. The porosity of the foam samples

are calculated by the equation shown below [62]: d; bulk density, Dr; density measured using helium

$$P = (1 - d/Dr).100 \quad (3.5)$$

In this study, Quantachrome Ultrapycnometer 1000 is used.

4. RESULTS AND DISCUSSIONS

In this section the effect of temperature, polymer addition and pressure on properties of carbon foam are discussed. In each case first the experimental results are given, the results are evaluated and comparisons are made with the available literature data.

4.1 The Effect of Temperature on the Foam Structure

In this part, the effects of operating temperature on foam structure are investigated. Three operating temperature of 300 ^{o}C, 350 ^{o}C and 450 ^{o}C are selected for the investigation of the effect of the temperature on carbon foam structure. The choice of these temperatures was based on previous study reported by Ekşilioğlu [63], and going beyond the limit of this study. Figure 4.1 gives the SEM images of the carbon foam samples obtained at three different temperatures.

The SEM photographs of the foam produced at 300 ^{o}C are given in the Figure 4.1a. In the same figure; b and c are the SEM photographs of the foams produced at 350 ^{o}C and 450 ^{o}C respectively.

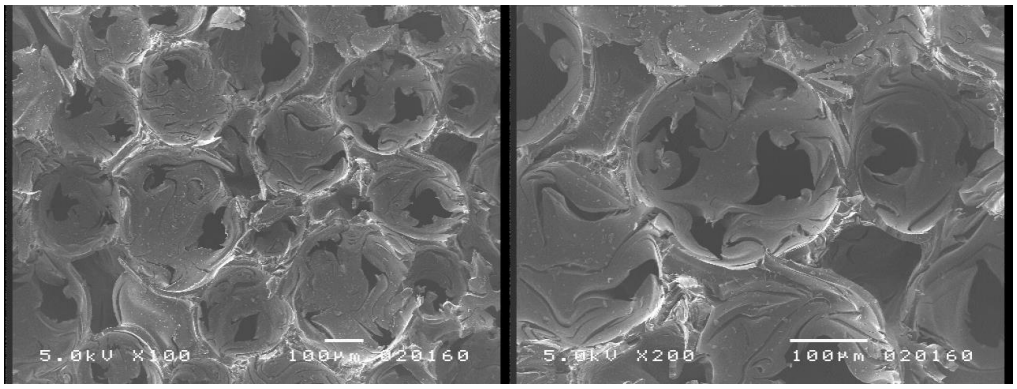

(a)

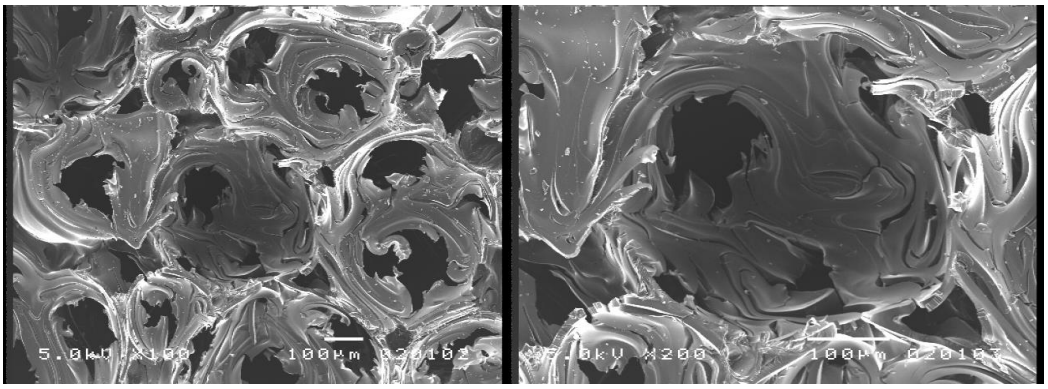

(b)

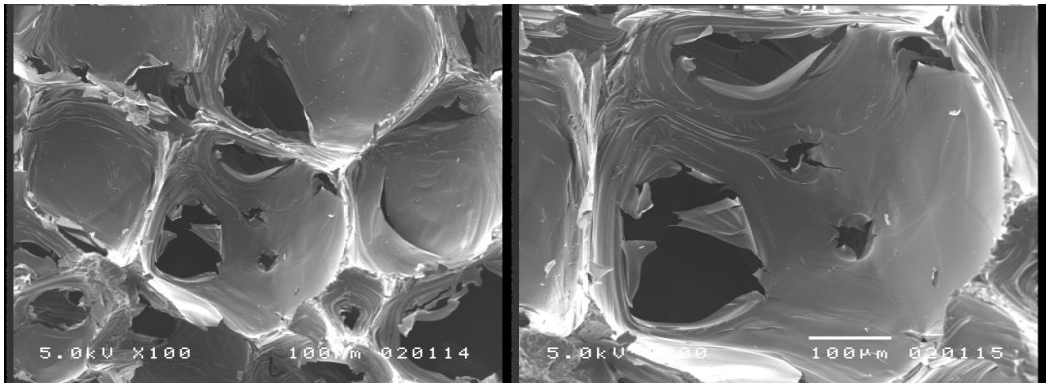

(c)

Figure 4.1 SEM photomicrographs of foam produced at different temperatures (all samples carbonized at 1050 ^{o}C) (a) T=300 ^{o}C, (b) T=350 ^{o}C, (c) T= 450 ^{o}C

From the SEM photographs, it is clear that the foam produced at 300 ° C has a well formed cell structure with evenly distributed rather uniform circular pores interlinking the adjacent cells. Ligaments, junctions and walls are well formed and surfaces are rather uniform. At the temperature of 350 ° C, the cell structure

deteriorated such that the cell is distorted from spherical geometry, ligaments, junctions and wall formation weakened and interconnecting pores are reduced in number, increased in size and deformed from circular geometry. At the highest temperature the structural deformation continued. It is noted in literature [49, 64-68] that the alignment of ligaments, junctions and cell walls are due to generated stress by the evolving volatiles at moderate temperatures and pressures. This is well illustrated with the processing envelope given for the mesophase pitch used in this study as shown in Figure 3.3.

As temperature is increased from 300 ° C to 350 and 450 ° C, the volatile matter evolution and gas mobility are increased. At the same time, the viscosity of the pitch decreased. Medium has fewer propensities to withstand to the stress generated by the volatiles. In other words the mesophase pitch becomes too fluid to retain the bubble shape imposed by the volatiles. As a consequence of these the deteriorations in cell, ligament, wall and interconnecting pores geometry and structure has taken place at the higher temperatures.

The starting point of foaming is the softening temperature of the pitch [63]. In literature operating temperature of the carbon foam is reported to be around 10-40 ^{o}C above the softening temperature [11, 10]. In this study the best foam formation was achieved at the temperature of 300 ^{o}C. This judgment is based on the investigation of scanning electron microscopy photographs which gives clear information on the formation of cells, ligaments, junction and general structure.

4.2 The Effect of Polymer Additives on the Foam Structure

In this part of the experiments, polymers like Polymethyl methacrylate (PMMA) and PS Polystyrene (PS) are used as additives at various ratios in order to investigate the effect of additives on carbon foam structure and properties. The optimum process conditions used in these experiments are 300 ^{o}C, 68 bars and 5 seconds pressure release time.

The SEM photographs of foams produced without additive is illustrated in Figure 4.2a. In this figure, b and c represent the foams with 10 % PMMA and 30 % PMMA additives respectively.

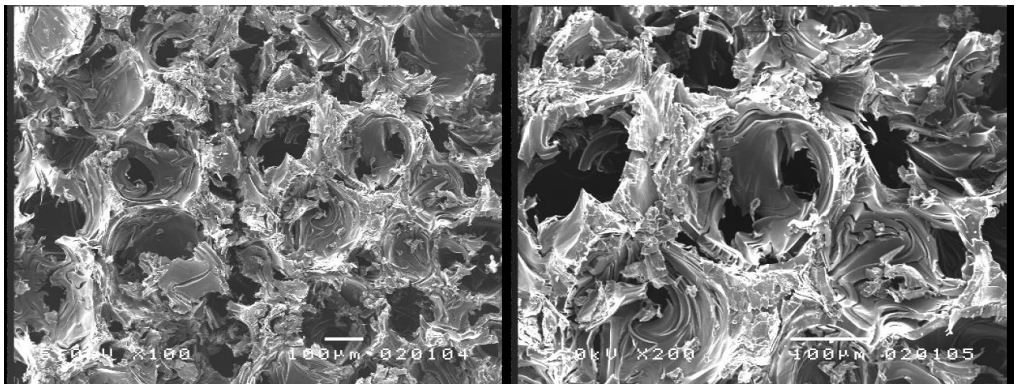

(a)

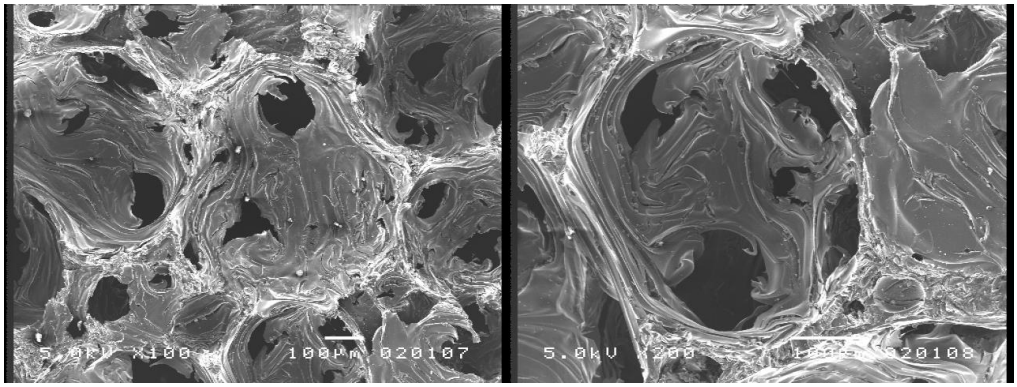

(b)

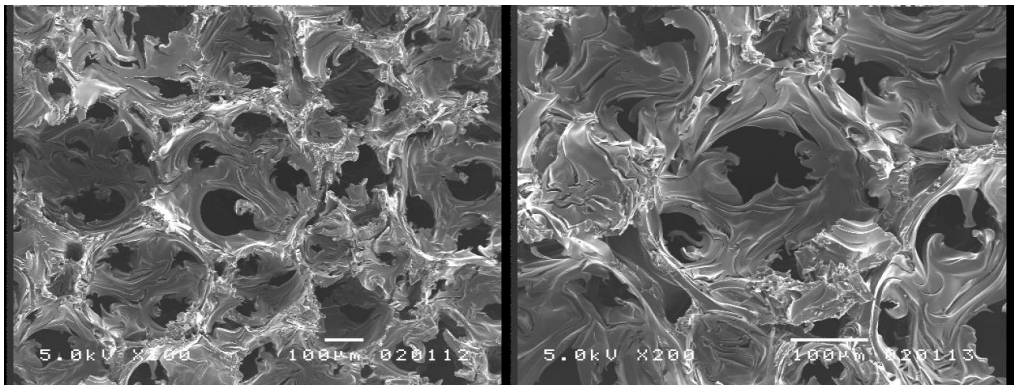

(c)

Figure 4.2 SEM images of foam with 10 % and 30 % PMMA additive and the foam produced without additive (all samples are graphitized at 3000 ^{o}C)

The number of the formation of cell and interconnected pore increases with the addition of the PMMA. As it can be seen from the SEM images of surface of carbon foam produced without polymer addition shows stacked planes, irregular flakes, and fibers. These textures seem to be modified towards a comparatively less rough surface. This suggests that there is some degree of surface modification as a result of

PMMA addition. Generally speaking, a more uniform structure is achieved. In previous studies on additives such as graphite, isotropic pitch and different solvents, a distinct deterioration of carbon foam structure was observed at the carbonized stage [63]. The results obtained in this study shows that PMMA addition is compatible in terms of cell, ligament, and wall. Also, pore formation evaluate at the end of graphitization stage. This result should be evaluated with respect to some measured characteristics.

The scanning electron photographs of foam produced without PS additive are shown in Figure 4.3a. In this figure, a and b represent the scanning electron photographs of foam produced with 20% and 30% PS additive respectively.

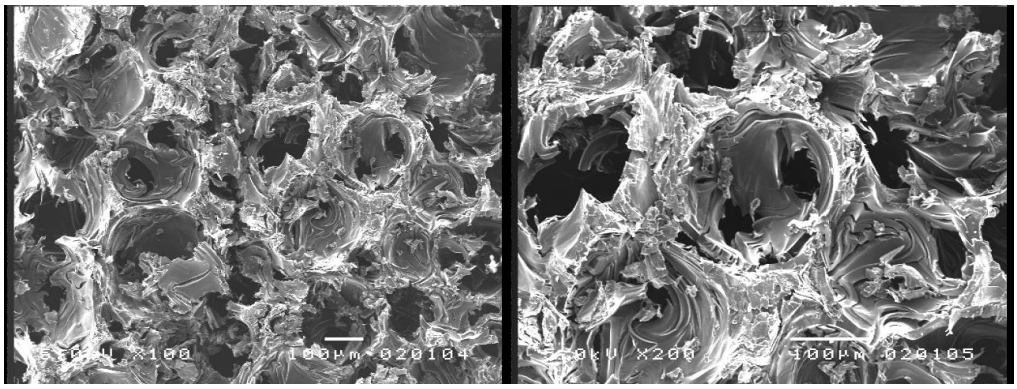

(a)

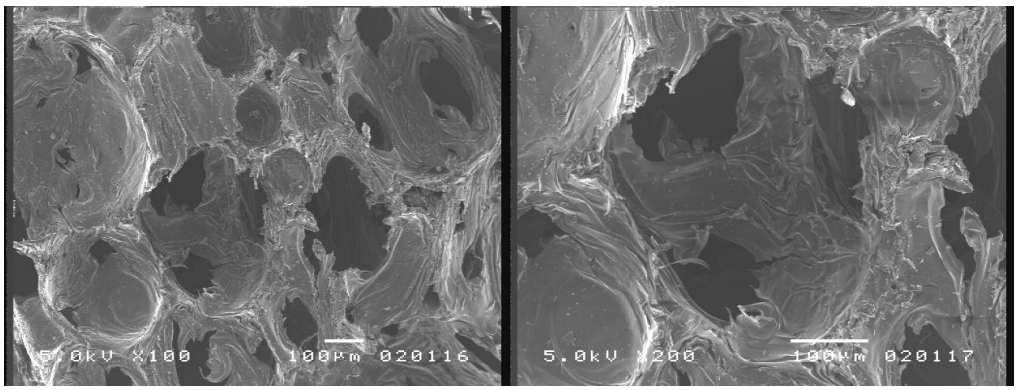

(b)

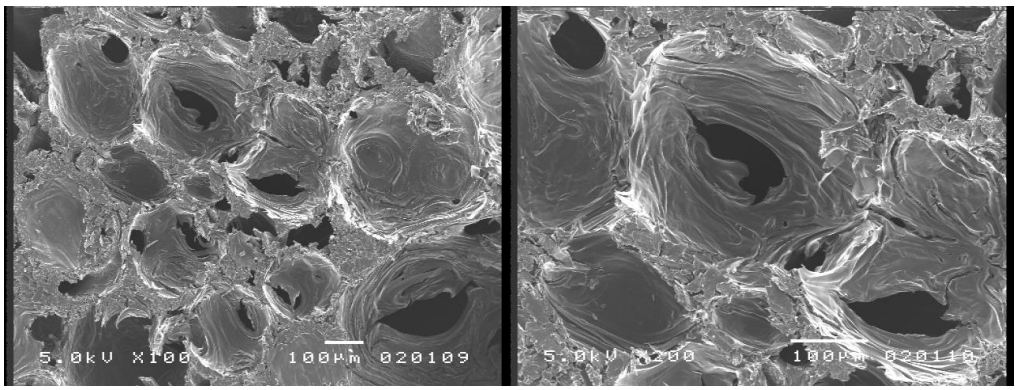

(c)

Figure 4.3 SEM images of foam with 20 % and 30 % PS additive and the foam produced without additive (all samples are graphitized at 3000 ^{o}C)

As it can be seen from Figure 4.3, beside the surface modification effect due to PS addition, there is also deterioration in the foam formation much more effective than the case of the PMMA addition. The formations of spherical cells are not fully realized.

The boundaries are not clear between the cells and the formation of ligaments and junctions are not completed. Another observation is that the pores are in less number at PS addition. In addition some areas having defects and non porous structure are observed.

4.3 The Effect of Pressure on Properties of Graphitized Carbon Foam

Green carbon foam samples were produced at various operating pressures of 38, 48, 58, 68 and 78 bar at constant temperature (300° C) and pressure release time of 5 sec. Further these carbon foams were stabilized, carbonized and graphitized. The quality of carbon foam products obtained at 38 and 48 bars are poor therefore the discussions and presentations are given for 58, 68, 78 bars only.

The scanning electron microscopy photographs of the graphitic carbon foams produced at three different pressures are given in Figure 4.4. In this figure; a, b, c are the SEM photographs of the foams produced at 58, 68 and 78 bars respectively.

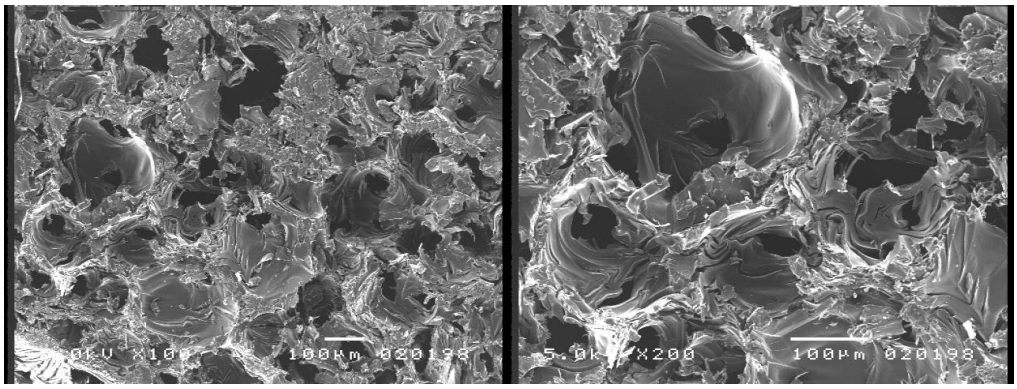

(a)

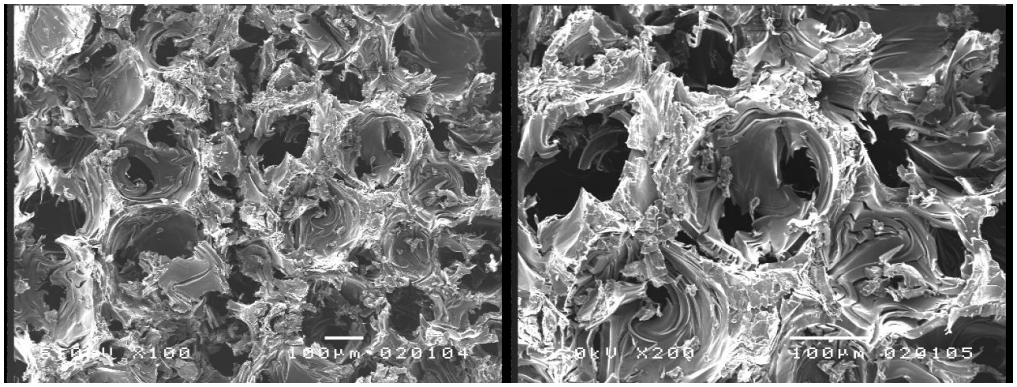

(b)

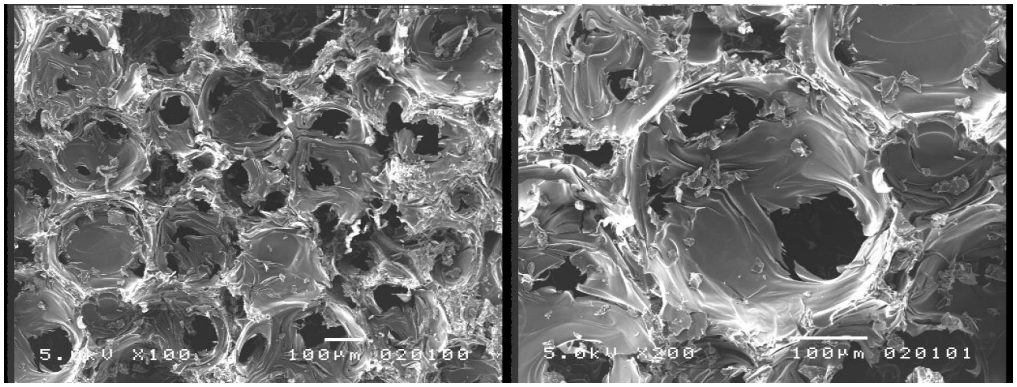

(c)

Figure 4.4 SEM photographs of carbon foam produced at various pressures experiments (a) P= 58 bar, (b) 68 bar, (c) 78 bar

It is evident from the images at Figure 4.4a that the formation of the cells is not well developed for 58 bars and there are few non spherical cells formed. Also interconnections of the cells are very poor. The non uniform and less ordered graphitic structure is observable. Low pressure is believed do not provide sufficient stress affect on the formation of cells. In a way that alignment of the rod-like

mesophase molecules at the bubble grown and pressure release stage is not sufficient. As it can be seen from the Figure 4.4b, the number of the cell and pores are increased and their geometry are more spherical compared to the carbon foams obtained at low pressure. Carbon foam produced at 78 bars shows spherical cells with interconnected pores which are seen from the SEM photographs in Figure 4.4c. The number of the cells as well as the pores increased compared to foam produced at 58 and 68 bar. Moreover ligaments between the pores are indication of better alignment of the mesophase molecules.

The skeletal densities of the foams are measured by Helium pycnometry. Total percentages of the carbon foam produced at different operating pressure are measured by using Equation 3.5. The skeletal density and the total porosity are 2 g/cm^3 and 74.8 % respectively for foams produced at 68 bar. This value is in reasonable agreement with the values reported in literature. Klett and co-workers [26, 27, 28, 29] reported 73-85 % porosity for the graphitized carbon foam produced from mesophase pitch. In a previous study Gencay [68] reported that porosity of carbonized carbon foam changed between 69-86% with applied pressures of 38 and 78 bars

The x-ray results of the different foam sample produced in this study and some other materials reported in literature that are compiled Table 4.1. The interlayer spacing calculated with Brag equation (Equation 3.3). The crystal size and stacking height are calculated by Scherrer equation (Equation 3.4).

Table 4.1 Comparison of X-Ray diffraction results and the degree of graphitization of carbon foam samples produced at different pressures, various carbon fibers and foam

Carbon Materials	Interlayer spacing d_{002} (nm)	Stack Height L_c (nm)	Crystal size L_a (nm)	gp* (%)
Graphitized carbon foam produced at 58 bar	0.3375	29.16	23.30	76
Graphitized carbon foam produced at 68 bar	0.3375	31.40	28.40	76
Graphitized carbon foam produced at 78 bar	0.3379	31.40	26.52	71
Mitsubishi ARA24 Foam-A[20]	0.3364	48,2	11.8	88
Mitsubishi ARA24 Foam-B[20]	0.3362	46,6	17.8	90
Conoco Foam-A[20]	0.3369	29,5	16.7	83
Conoco Foam-B[20]	0.3366	38,7	13	86
Clemson Ribbon[20]	0.3369	19	62	83
K1100[20]	0.3366	62	109	86
Pitch Fiber[20]	0.3364	66	102	88
Fixed catalyst VGCF[20]	0.3366	37	40	86

*gp= degree of graphitization and is defined as (0.3440-d_spacing)/(0.3440-0.3354) where 0.3440 and 0.3354 are the d_spacing of turbostratic graphite and single crystal (perfect) graphite[66]

Carbon foams produced at 58 and 68 bars have interlayer spacing of 0.3375 nm. Also the interlayer spacing of carbon foam obtained at 78 bar is 0.3379 nm. These values are close to pure graphite value (0,3354nm). The crystal size in c-direction (L_c) ranged from 29.16 to 31.4 nm and the crystal size in a-direction (L_a) ranged from 29.16 to 31.4. These crystal sizes are similar to other reported value in the literature[20, 52, 66-68]. Table 4.1 shows that crystal sizes in both directions are similar to high thermal conductivity carbon fibers and other kind of carbon foam. In addition, carbon foams produced at different pressures have similar graphitization degree to other types of carbon foams and fibers.

The thermal conductivity of the carbonized foams is very low at the level of 1-2 W/m.K [20]. After graphitization, the thermal conductivity of the foams is reported to be between 0.4-210 W/m.K [69-72]. Thermal conductivity of foams is managed by lattice vibration as mentioned in section 2.7.2.6. Foam produced 58 bar have lower crystal size in c direction, so lattice vibrations are relatively small. Also examination of SEM photographs demonstrated that the interconnected structure and pore formation of foams are comparatively weaker than the other foam produced at 68 and 78 bars. Therefore the thermal conductivity measurement is not performed for this carbon foam sample. Thermal diffusivities of the samples are measured by LFA 427 apparatus. Later, thermal conductivities of the foams are calculated by Equation 3.1. Thermal conductivities of the foam produced at 68 and 78 bars are 36.6 W/m.K and 23.6 W/m.K respectively. Decrease in conductivity may be explained by preferred orientation of the foams amples. Foam produced at 68 bars has low d-spacing and high crystallite size compared to foam produced 78 bar. Therefore heat transfer and lattice vibration is relatively higher for the former one. Consequently foam produced at 68 bars has higher thermal conductivity.

Thermal conductivity of the foams are calculated for different temperatures and shown in Figure 4.5. While temperature increases, matching with the defects and the probability of collision between the phonons increase. Defects and interactions disrupt thermal conductivity. Defects cause interruption of phonons vibration. Interactions between the phonons impede vibration of lattice. While temperature increases. As a result, thermal conductivity decreases when temperature increases.. This is expected and common behavior for all graphite's.

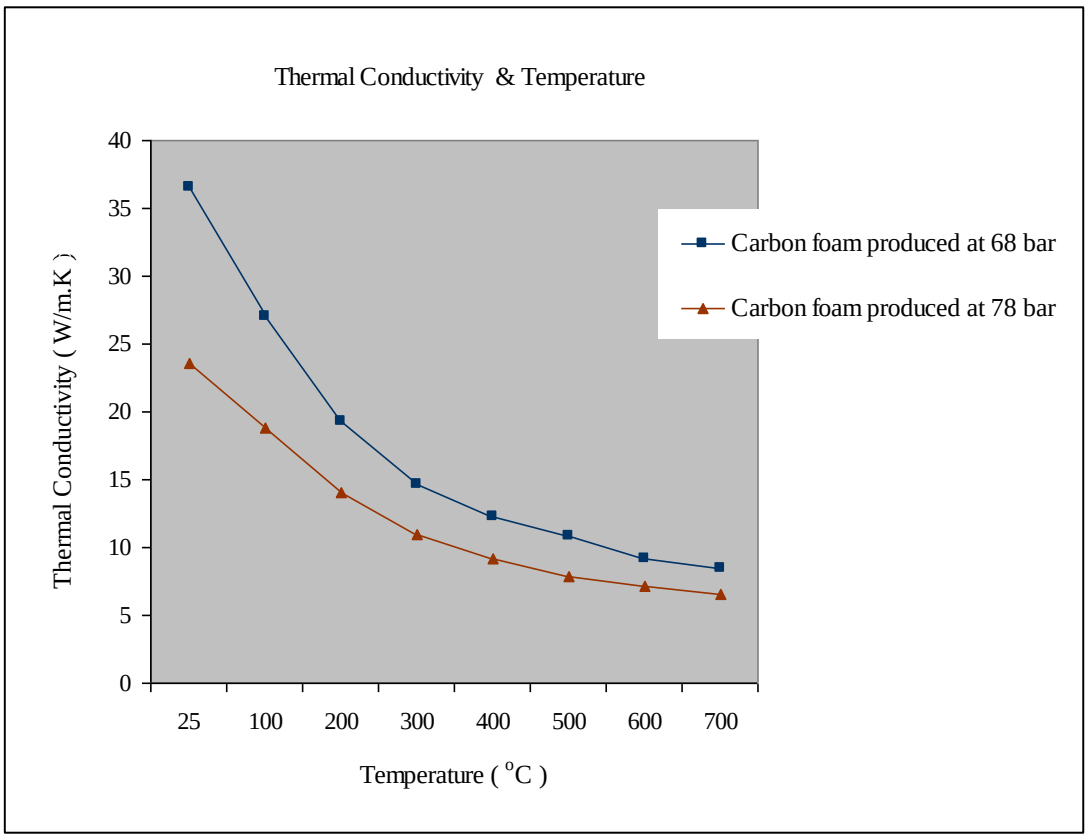

Figure 4.5 Thermal conductivity of foams according to the temperature

The thermal conductivity of the foam samples with the various carbon foams are shown in Table 4.2. Produced carbon foam samples have higher thermal conductivity than Touchstone, Ultramet, first Mer Foam. But the thermal conductivity of the foams studied is well below from the conductivity values of other Mer's and Ornl's Foams.

Table 4.2 Thermal conductivity of carbon foams produced and different kind of carbon foams

Material	Density (g/cm^3)	Thermal Conductivity W/m K
Carbon foam produced at 68 bar	0.54	36.60
Carbon foam produced at 78 bar	0.48	23.60
Touchstone[69]	0.16	0.40
Touchstone[69]	0.16	13.90
Touchstone[69]	0.40	0.80
Touchstone[69]	0.40	17.50
Ultramet [70]	0.04	0.09
Mer [71]	0.02	0.05
Mer [71]	0.16	50.00
Mer [71]	0.32	150,00
Mer [71]	0.42	180.00
Mer [71]	0.62	210.00
Ornl foamI [72]	0.26	50.00
Ornl foamI [72]	0.47	107.30
Ornl foamI [72]	0.52	120.70
Ornl foamI [72]	0.60	132.90
Ornl foamII [72]	0.31	41.50
Ornl foamII [72]	0.35	56.10
Ornl foamII [72]	0.43	86.60
Ornl foamII [72]	0.59	135.40
Ornl foamIII [72]	0.67	147.60
Ornl foamIII [72]	0.69	163.90
Ornl foamIII [72]	0.70	178.50

The thermal properties of aluminum and copper and studied carbon foams are given Table 4.3. Specific thermal conductivity of foams produced at 68 bar is higher than the values of aluminum and copper. The thermal conductivity of the foam produced at 78 bar is between the values of copper and aluminum

Table 4.3 Thermal properties of foams produced, copper and aluminum

Material	Density (g/cm^3)	Thermal Conductivity (W/m.K)	Specific Thermal Conductivity*
Carbon Foam produced 68 bar	0.54	36.60	67.80
Carbon Foam produced 78 bar	0.48	23.60	49.20
Copper	8.90	400	44.94
Aluminum	2.77	150	54.15

* Specific thermal conductivity = thermal conductivity / density

5. CONCLUSIONS

In this study, the effect of temperature on the properties of carbonized foam is investigated. In addition, the effect of PMMA and PS addition on the properties of graphitized foam structure is studied. Furthermore, the effect of pressure on the properties of graphitized carbon foam is examined. The results are concluded as follows;

1. Carbon foams obtained at temperatures higher than 300 ^{o}C resulted in poorer foam formation, indicated as deterioration in the cell, ligaments, junctions and wall formation and structure in general.
2. PMMA and PS additions to mesophase pitch resulted in smoother carbon foam topography. This structural change was accomplished with loss of foaming quality for the case of PS addition compared to PMMA.
3. In terms of structural parameters of interlayer spacing, stack height, crystal size and graphitization degree of graphitized carbon foam that is obtained at 68 bar pressure, 300 ^{o}C temperature and 5 seconds pressure release time resulted in better graphitic structure.
4. The highest specific thermal conductivity result is obtained for graphitized carbon foam obtained at 68 bar pressure, 300 ^{o}C temperature and 5 seconds in this study.

6. RECOMMEDATIONS AND FUTURE WORK

Investigation and characterization of graphitized and carbonized foam under different process conditions is studied. As a result of the findings of this study following research topics may be considered for further investigation:

1. To modify process conditions in order to widen application areas enable to tailor foam for specific applications.
2. To reduce the process steps in order to improve economic feasibility of the process.
3. Increase the thermal properties in order to improve the standing of the product of continuing study among the referred material reported in the thesis.
4. To investigate the affect of different kinds of polymer on the foam structure and properties.

REFERENCES

[1] **Ford, W,** 1964. Method of Making Cellular Refractory Thermal Insulating Material, *United States Patent*, No: 3121050.

[2] **Marsh, H,** 1997, Carbon materials: an overview of carbon artifact, *Introduction to Carbon Technologies*, pp 1-34, Eds. Marsh, H, Heintz, E.A., and Rodriguez-Reinoso, F., Universaded de Alicante, Secretariade de Publicaciones.

[3] **Savage. G,** 1993, *Carbon Carbon Composites*, pp1-10, Chapman&Hall, London, UK

[4] http:// www.edinformatics.com/math_science/c_atom.htm dated December 1, 2004.

[5] **Burchell, T**, 1999, Structure and Bonding in Carbon Materials, *Carbon Materials for Advanced Technologies*, p1-29, Amsterdam, New York, Pergamon.

[6] http://en.wikipedia.org/wiki/Diamond dated December 1, 2004.

[7] http://home.att.net/~cat6a/allot_carbon-I.htm dated December 1, 2004.

[8] http://dendritics.com/scales/c-allotropes.asp dated December 1, 2004.

[9] **Marsh, H,** 2000, Structure in Carbons and Carbon Artifacts, *Science of carbon materials*, pp1-90, Eds: Marsh, H, Rodriguez-Reinoso, F., Universaded de Alicante, Secretariade de Publicaciones.

[10] **Marsh, H,** 1989, Carbon Forms, *Introduction to Carbon Science*, pp10-15, Butterworth&Co. Ltd, England.

[11] **Kearns, K M,** 1999. Pitch foam products, *United States Patent*, No: 5961814 dated October 5, 1999.

[12] **Murdie N, Parker, C A, Pigford, J. F., Narasimhan, D, Dillon, F.**, 2000. Process of making carbon-carbon composite material made from densified carbon foam, *United States Patent*, No: 6077464 dated June 20, 2000.

[13] **Bonzom, A, Crepaux A.P., Moutard, A E. J.,** 1981. Process for preparing pitch foams and products so produced, *United States Patent*, No: 4276246 dated June 30, 1981.

[14] **Stiller, A H, Stansberry, P. G, Zondlo J. W,** 2002. Method of making a carbon foam material and resultant product, *United States Patent*, No: 6346226 dated February 12, 2002.

[15] **Simandl, R F., Brown, J. D.,** 1994. Microcellular carbon foam and method, *United States Patent*, No: 5300272 dated April 5, 1994.

[16] **Vinton, C S., Franklin, C. H.,** 1977. Method for the preparation of vitreous carbon foams, *United States Patent*, No: 4022875 dated May 10, 1977.

[17] **Raley, Jr., Charles, F., Asher, D R,** 1976. Process for preparing macroporous open-cell carbon foam from normally crystalline vinylidene chloride polymer, *United States Patent*, No: 3960770 dated June 1, 1976.

[18] **Hopper, R W, Pekala, R W,** 1988. Low Density Microcellular Carbon or Catalytically impregnated carbon foams and process for their preparation, *United States Patent*, No: 4756898 dated July 12, 1988.

[19] **Reznek, S. R, Massey, R K,** 2002. Carbon foams and methods of making the same, *United States Patent*, No: 6500401 dated December 31, 2002 dated December 31, 2002.

[20] http:// www. ms. ornl. gov/ott/publications/sampe98.pdf dated December 5, 2004.

[21] **Klett, J., Hardy, R, Romine, E, Walls, C, Burchell, T.,** 2000. High-thermal-conductivity, mesophase-pitch-derived carbon foams: effect of precursor on structure and properties, *Carbon*, **38**, 953-973.

[22] **Klett, J.,** 2001. Pitch-based carbon foam and composites, *United States Patent*, No: 6261485 dated July17, 2001.

[23] **Luhleich, H, et. al.**, 1975. Method of making carbonaceous bodies, *United States Patent*, No: 3927187 dated December 16, 1975.

[24] **Vinton, C, Franklin, C.,** 1975. Method for the preparation of carbon structures, *United States Patent*, No: 3927186 dated December 16, 1975.

[25] **Kearns, K M,** 1999. Process for preparing pitch foams, *United States Patent*, No: 5868974 dated Februray9, 1999.

[26] **Googin, J., Napier, Scrivner, J. M,** 1967. Method for manufacturing foam carbon products, *United States Patent*, No: 3345440 dated October 3, 1967.

[27] **Klett, J., Burchell, T.,** 2002. Pitch based carbon foam heat sink with phase change material, *United States Patent*, No: 6399149 dated June 4, 200

[28] **Klett J. W,** 2000. Method for extruding pitch based foam, *United States Patent*, No: 6344159 dated February 5, 2002.

[29] **Klett J. W,** 2000. Process for making carbon foam, *United States Patent*, No: 6033506 dated March 7, 2000.

[30] **Mochida, I., Korai, Y., Ku, C., Watanabe F., Sakai, Y., 2000**. Chemistry of synthesis, structure, preparation and application of aromatic-derived mesophase pitch, *Carbon*, **38**, 305-328.

[31] **Kearns, K. M.,** 1999. Process for preparing pitch foams, *United States Patent*, No: 5868974 dated February 9, 1999.

[32] http://www.mgc-a.com/newProducts/media/ARBrochure.pdf dated December 5, 2004.

[33] http://acs.omnibooksonline.com/papers/1995_46.pdf dated December 5, 2004.

[34] **Marsh, H**, 2000. Tar and pitch: composition and application, *Science of Carbon Materials*, pp173-203 Eds. Menendez, R, Bermejo, J., Fiqueiras, A., Universaded de Alicante, Secretariade de Publicaciones.

[35] http://www.ms.ornl.gov/researchgroups/CMT/FOAMoverview.pdf dated December 5, 2004.

[36] **Blanco, C., Lu, S., Appleyard, S. P., Rand, B., 2003.** The stabilisation of carbon fibres studied by micro-thermal analysis, *Carbon*, **41**, 165–171.

[37] **Drbohlav, J., Stevenson W. T. K.** 1995. The Oxidative stabilization and carbonization of a synthetic mesophase pitch, part I: the oxidative stabilization process, *Carbon*, **33(5)**, 693-711.

[38] **Lavin, J. G.,** 1992. Chemical reactions in the stabilization of mesophase pitch-based carbon fiber, *Carbon*, **30(3)**, 351-357.

[39] **Fanjul, F., Granda, M., Santamaría, R., and Menéndez, R**, 2002. On the chemistry of the oxidative stabilization and carbonization of carbonaceous mesophase, *Fuel*, **81**, 2061-2070.

[40] **Liedtke, V., Hüttinger, K. J.,** 1996. Mesophase pitches as matrix precursor of carbon fiber reinforced carbon: II. Stabilization of mesophase pitch matrix by oxygen treatment, *Carbon*, **34(9)**, 1067-1079.

[41] **Yoon, S., Korai, Y., Mochida, I.,** 1994. Assessment and optimization of the stabilization process of mesophase pitch fibers by thermal analyses, *Carbon*, **32(2)**, 281-287.

[42] **Drbohlav, J., Stevenson, W. T. K.** 1995. The oxidative stabilization and carbonization of a synthetic mesophase pitch, part II: the carbonization process, *Carbon*, **33(5)**, 713-731.

[43] **Oshida K, Bonnamy S., 2002.** Primary carbonization of an anisotropic mesophase pitch compared to conventional isotropic pitch, *Carbon*, **40**, 2699-2711.

[44] **Miura, K, Nakagawa, H, Hashimoto, K,** 1995. Examination of the oxidative stabilization reaction of the pitch-based carbon fiber through continuous measurement of oxygen chemisorption and gas formation rate, *Carbon*, **33 (3)**, 275-282.

[45] **Liedtke, V., Hüttinger, K. J.,** 1996. Mesophase pitches as matrix precursor of carbon fiber reinforced carbon part II: stabilization of mesophase pitch matrix by oxygen treatment, *Carbon*, **34(9)**, 1067-1079.

[46] **Rogers, D. K, Plucinski, J. W,** 2003. Coal-based carbon foam, *United States Patent*, 6656238 dated December 2, 2003.

[47] **Pierson, H O,** 1993. Carbons as an element, *Handbook of carbon, graphite, diamond, and fullerenes*, Noyes Publications, pp 1-44, Noyes Publications, USA

[48] http://www.ms.ornl.gov/researchgroups/CMT/FOAM/klett-jmatsci-2003.pdf

[49] **Savage, G,** 1993. The properties of carbon carbon composites, *Carbon Carbon Composite*, pp277-317, Chapman&Hall, USA,.

[50] **Turton, R,** 2000. Thermal Properties, *The Physics of Solids*, pp 183-208, Oxford University Press, USA

[51] **Gallego, N, Klett, J., Walls, C., McMillan, A,** 2003., The role of structure on the properties of graphitic foams, Oak ridge national laboratory internal report, USA

[52] http://www.ms.ornl.gov/researchgroups/CMT/FOAM/one-pagers.pdf dated December 5, 2004.

[53] http://www.ornl.gov/info/ornlreview/v35_3_02/tool.shtml dated December 5, 2004.

[54] http://www.ornl.gov/info/ornlreview/v35_3_02/v35_no3_02review.pdf dated December 5, 2004.

[55] **Patel, N, Okabe, K, Oya, A**, 2002. Designing carbon materials with unique shapes using polymer blending and coating techniques, *Carbon*, **40**, 315-320

[56] **Hulicova, D, Oya, A,** 2003. The polymer blend technique as a method for designing fine carbon materials, *Carbon*, **41**, *1443-1450*

[57] **ASTM C-781-96**, 1999. Boronated graphite components for high temperature gas cooled nuclear reactors, USA

[58] http://www.ms.ornl.gov/htmlhome/tpuc/l-flash.html dated December 5, 2004.

[59] **Lifshin, E,** 1999. *X-ray Characterization of Materials*, Wiley-VCH, Germany.

[60] **Suryanarayana, C, Norton, G M,** 1998. *X-ray Diffraction: a practical approach*, Plenum Press, USA

[61] **Savage, G,** 1993., *Carbon Carbon Composites*, pp13-26, Chapman&Hall, London, UK

[62] **Kanno, K, Tsuruya, H, Fujiura, R, Koshikawa, T., Watanabe, F.,** 2004. *Carbon foam*, graphite foam and production processes of these, United *States Patent*, 6,689,336 dated February 10, 2004.

[63] **Ekşilioğlu, A,** 2003. Effect of temperature, solvent type, and additives on the properties of mesophase pitch, M.Sc. Thesis, ITU, Institute of Science and Technology, Istanbul.

[64] **Klett, J., Mcmillan, A, Gallego, N Gallego, G, Walls, C,** 2003. Effect of heat treatment conditions on the thermal properties of mesophase pitch derived graphitic foams, Oak ridge national laboratory, Metals and ceramics division internal report, USA

[65] **Klett, J., Mcmillan, A., Gallego, N. Gallego, G., Walls, C.,** 2003. Effect of heat treatment conditions on the thermal properties of mesophase derived graphitic foams, Oak ridge national laboratory, Metals and ceramics division internal report, USA.

[66] **Klett, J.,** 1998. High thermal conductivity, mesophase pitch derived carbon foam, Proceedings of the 43rd International SAMPE Symposium, May 31-June 4, Anaheim, California.

[67] **Murdie, N., Parker, C. A., Pigford, J. F., Narasimhan, D. Dillon, F.,** 2002. Process of stabilizing carbonaceous pitch-based foam, *United States Patent*, 6342171, dated January 29, 2002.

[68] **Gencay, N.,** 2003, A mesophase pitch derived carbon foam: effect of pressure and release time, M.Sc. Thesis, ITU, Institute of Science and Technology, Istanbul.

[69] http://www.industrialheating.com/CDA/ArticleInformation/features/BNP__Features__Item/0,2832,87444,00.html dated December 5, 2004.

[70] http://www.ultramet.com/old/8.htm dated December 5, 2004.

[71] http://www.mercorp.com/mercorp/CGraphiteFoams/C_Graphite_Foams.html dated December 5, 2004.

[72] http://www.ms.ornl.gov/researchgroups/CIMTECH/foam/foams.htm dated December 5, 2004.

CURRICULUM VITAE

Ayşenur GUL was born in Istanbul, Turkey in 1978. She was graduated from Uskudar Science High School in 1996. She entered Istanbul Technical University Department of Chemical Engineering in 1997. After graduation as a chemical engineer in 2002, she started her M.Sc studied at Istanbul Technical University Department of Material Science and Engineering in the same year.